CO OXIDATION ON PALLADIUM USING MULTI-LATTICE KINETIC MONTE CARLO

MAX J. HOFFMANN

Diplomarbeit

Fachbereich Physik

Freie Universität Berlin

June 2010

Diese Arbeit wurde vom August 2009 bis Juni 2010 unter der Aufsicht von Prof. Dr. Karsten Reuter in der Theorieabteilung des Fritz-Haber-Institutes der Max-Planck-Gesellschaft durchgeführt.

Max J. Hoffmann: *CO Oxidation on Palladium Using Multi-lattice Kinetic Monte Carlo,* Diplomarbeit, © June 2010

SUPERVISORS:
Karsten Reuter
Matthias Scheffler

LOCATION:
Berlin

ABSTRACT

CO oxidation is probably the most widely studied chemical reaction in heterogeneous catalysis due to its eminent importance and its apparent simplicity.

Nevertheless, many fundamental aspects are still not understood. CO oxidizes under oxygen-rich conditions at transition metal surfaces. Accordingly it is being debated whether an oxide layer forms on the surface of the operating catalyst. These oxides typically do not exhibit the same lattice structures as the metallic substrate. This is a serious challenge for atomistic kinetic theories such as kinetic Monte Carlo. In the present study I develop a multi-lattice approach to address this limitation, using the example of CO oxidation on Pd(100).

ZUSAMMENFASSUNG

Die Oxidation von CO ist, aufgrund ihrer herausragenden Bedeutung und scheinbaren Einfachheit, vermutlich die am häufigsten untersuchte chemische Reaktion der heterogenen Katalyse.

Dennoch sind viele grundlegende Aspekte noch unverstanden. Kohlenstoffmonoxid oxidiert unter sauerstoffreichen Bedingungen an Übergangsmetalloberflächen. Folglich stellt sich die Frage, ob sich eine Oxidschicht auf der Oberfläche bildet. Solche Oxide weisen typischerweise eine andere Gitterstruktur auf als das metallische Substrat, was für atomistische, kinetische Methoden wie kinetisches Monte Carlo eine Herausforderung darstellt. In der vorliegenden Arbeit entwickele ich, am Beispiel von CO Oxidation auf Pd(100), einen mehrgittrigen Ansatz.

CONTENTS

ACRONYMS

DFT	density functional theory
kMC	kinetic Monte Carlo
MD	Molecular Dynamics
ml-kMC	multi-lattice kMC
TOF	turn-over-frequency

1 INTRODUCTION

1.1 HETEROGENEOUS CATALYSIS FROM 10,000 FEET

A substance that influences the rate of a chemical reaction without being consumed is said to be a catalyst. [1] Catalysts are a key element of many chemical processes that have significant influence on our everyday life such as ammonia synthesis or exhaust gas conversion. Also many envisioned schemes for energy storage and conversion include a catalyst, that yet has to be found, as a key element. [2]

Unfortunately in the past virtually all catalysts have been discovered empirically by means of trial-and-error. Many clever strategies have been developed to maximize the speed of this search but by and large it remains a very involved process and the knowledge from one working catalyst can rarely be transferred directly to another reaction. This motivated a long-term effort to develop a fundamental, atomic-scale understanding to eventually predict and design the behavior of catalysts. [3]

One differentiates between homogeneous and heterogeneous catalysts, depending on whether reactants and catalysts are in the same aggregate state or not. The latter type makes up the vast majority of technological applications but is also particularly challenging to understand conceptually.

One source of difficulties is a potentially complex geometry. In homogeneous catalysis one often strives to find the active site of a catalyst, which is said to be responsible for the catalytic activity. In heterogeneous catalysis this concept often does not apply because the activity is due to the delicate interplay of several sites. To have a common reference and to pave the road to a more systematic understanding one therefore focuses on smooth, well-defined single crystal surfaces. Even though technological catalysts feature very rough structures with extremely large surfaces areas one hopes conclusions can be drawn from such model catalysts. This hope is mainly based on the fact that microscopic particles display large facets of single crystal surfaces.

Closely related but on a different level are experimental challenges of heterogeneous catalysis. Classical surface science methods have been developed for ultra high vacuum conditions and low temperatures. Here dynamics are easier to control and interpret. However common technological catalysts perform under ambient or higher pressures and elevated temperatures. It has been recognized that the structures and mechanisms may differ significantly between vacuum and technologically relevant conditions. This fact is usually referred to as pressure gap. [4] However, the atomic-scale analysis at high pressure conditions to verify the existence of a pressure gap remains exceedingly challenging.

Another difficulty is the inherent multiscale character of the problem. The essential ingredients of catalysts are rooted in quantum mechanics on length scales of angstroms and times scales of femtoseconds. The behavior or functions one aims to predict exist only on

length scales of milliseconds and centimeters, respectively. To predict the lifetime or the influence of mass transfer effects one may even have to consider hours and meters. Multiscale problems are pervasive in real systems and the sheer number of approaches is a good indicator of its complexity. [5–7]

Progress in numerical techniques such as density-functional theory (DFT) has brought unprecedented insight to the microscopic picture of catalysts. [8, 9] A chemical reaction is a dynamic process thus knowledge of the ground-state electronic structure alone cannot provide a comprehensive description.

A promising method to link an atomistic description to a mesoscopic scale is kinetic Monte Carlo (kMC). To further its development we tackle a fairly simple reaction that is of fundamental interest but exceeds the current realm of applicability. The present example is CO oxidation on Palladium (100), which may exhibit more than one lattice-like geometry near reactive conditions.

1.2 ATOMISTIC VIEW OF HETEROGENEOUS CATALYSIS

1.2.1 *Setting the Scene*

A very powerful point of view on catalysis is a potential energy (hyper) surface (PES) formulation. The PES is the total energy of the system as function of all nuclei, *i.e.* of the combined system of reactant, catalyst, and product. A highly optimized coordinate for the problem at hand is the so called reaction coordinate, which characterizes positions of all relevant nuclei from initial state (reactants) to final state (products) with a single number (see figure 1). This reaction coordinate has to be thought to represent the movement of all interacting particles (reactants and a truncated environment of the catalyst) for this specific process. Also refer to the discussion of reaction path and transition state below.

Following this picture a PES has a maximum along the reaction coordinate and a chemical reaction means to cross this maximum. In practice the system can cross this barrier due to fluctuations of stochastic movements, *e.g.* vibrations, at elevated temperature. The role of a catalyst can be thought to modify the PES in such a way that the maximum between initial and final states or any two metastable intermediates is as low as possible.

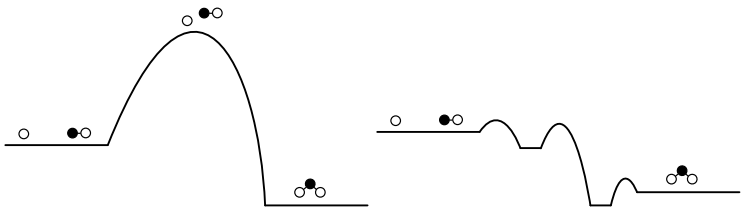

(a) without catalyst (b) with catalyst

Figure 1: A schematic view of the potential energy surface along a reaction coordinate for a simple chemical reaction.

So far so easy. In practice to map out this PES accurately is non-trivial but only one fragment of a full description of a working catalyst because the interplay between elementary steps needs to be taken into account as well. To understand what steps make up a successful

chemical reaction in a simple heterogeneous catalyst, we need to take a refined look.

In a heterogeneous catalytic system a reaction scheme could look as follows: The catalyst is some solid state material surrounded by reactants in gaseous form. For sake of simplicity we imagine this gas as some mixture of ideal gases. According to kinetic gas theory gas particles move through space with velocities given by the Maxwell-Boltzmann distribution. [10] When particles encounter a solid surface the direction of the velocities is reversed but speed is unchanges (an elastic collision). Strictly speaking this is not always the case but the particle may stick to the surface of the catalyst due to a chemical bond. One says the molecule adsorbed on the surface. On an atomic scale this typically does not happen at arbitrary locations on a solid state material but at discretely distributed spots due to it crystalline structure. Consequently such a site is said to be an adsorption site. An adsorption site that is occupied by a particle now has an altered PES for surrounding particles. In many cases of heterogeneous catalysts the probability that two particles adsorb on top of each other is so low, that from now on we assume only a monolayer of adatoms blocking further adsorption once a site occupied. Of course this does not have to be true for every catalyst and every species.

Once on the surface a particle can hop to other adsorption sites in the vicinity, in which case the particle is said to diffuse on the surface. The particle can also overcome the local minimum in other directions and hop back into the gas phase, which is called desorption. By far the longest time though the particle simply oscillates around a PES minimum. This is one important source of multiple time scales. Another one is that under identical conditions some elementary steps may occur more often than others by orders of magnitude.

For our simple catalyst the most desirable direction would be if the particle comes to rest next to another reactant, either by diffusion or adsorption, and forms a chemical bond with it, when particles are said to react with one another. As a final step this new particle needs to desorb from the surface. The reaction scheme described here comes under the name of Langmuir-Hinshelwood kinetics [4] and is the only one considered in this study.

Returning to our PES picture a reactive heterogeneous catalyst needs to provide among other things for low barriers for each of the elementary steps: adsorption, diffusion, reaction, and desorption.

1.2.2 *Other Reaction Mechanisms*

The simple reaction scheme includes only one way how particles can react with one another and it is the only reaction type considered in the model developed later. Other reaction types are possible and have been discussed in the past. Most notable are scattering reactions (also called Eley-Rideal reaction [4]) where an impinging particle reacts immediately with a particle bound to the surface. A simple argument questioning a significant relative contribution from Eley-Rideal reactions is that rate constants are bound by the impingement rate of gas molecules ($\sim 10^8 \mathrm{s}^{-1}\mathrm{site}^{-1}$ at room temperature and ambient pressures) whereas surface-surface mechanisms are bound by the frequency of atomic vibrations ($\sim 10^{13}\mathrm{s}^{-1}\mathrm{site}^{-1}$ at room temper-

ature). [11] However if we look at high pressures one might want to re-estimate this approximation.

1.2.3 *Discussion of the Reaction Coordinate Picture*

In the beginning of this section we simply used a reaction coordinate to describe a system's location in phase space between initial and final state. As one can imagine on a real surface this path can quickly resemble a complex graph in terms of intermediate states and transitions.

First we must require that the PES exhibits distinct local minima so that the initial states resemble points in phase space. This is usually given if a particle is said to chemisorb [4] on the surface. Then at this point it is worth to introduce the concept of a transition state. A transition state is defined as the state with the highest energy along the transition path. This state is a saddle point on the PES between two local minima since the reaction typically crosses the lowest barrier (see also figure 2). This is of course only a valid picture if the PES has a smooth shape with one somewhat distinct saddle point. For more crumbled surfaces more transition states might have to be considered and weighted appropriately. Also for processes like adsorption there is often no obvious transition path at all.

In either case a transition state is chronically elusive to *in situ* experiments under most reactive conditions since the system spends much less time in this state than in most other states and theoretical predictions are difficult to validate directly.

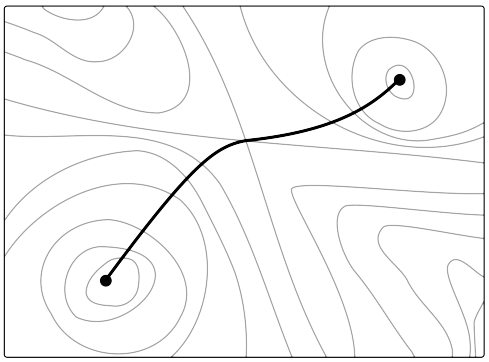

Figure 2: Schematic sketch of PES and reaction path. The highest point along the reaction path is a saddle point of the PES.

1.2.4 *Sabatier Principle*

The reaction scheme so far is very simple and many complications have been left out. However it suffices to illustrate an important constraint a PES of a working catalyst must fulfill. In anticipation of section 2.5 we note that a transition rate of a process tends towards zero if the energy difference between final state and initial state is much larger than the average thermal energy carried by a particle ($\sim k_B T$).

Applied to our reaction scheme one can conclude that a particle needs to bind strong enough to the surface so that the time spent on the surface is large enough to have a chance to react. On the other hand products needs to bind weak enough, so that they desorb quickly from

the surface. This general qualitative rule is known as Sabatier principle. [4]

This crucial observation has led to approaches, where only such energy differences where considered to estimate the reactivity of a catalyst. [12] It is easy to see that this is not a reliable descriptor for all catalysts at arbitrary conditions. Many other factors can hinder surface chemical reactions. At ambient pressures we observe that most metal surfaces are fully covered by adatoms of some species within a fraction of a second. So the number of incoming particles on the catalyst is limited by the fraction of empty adsorption site, rather than the impingement rate of gas particles.

1.2.5 *Other Properties of Interest*

The given reaction scheme aims to explain the reactivity of a catalyst. A given catalysts however not only needs to be reactive towards a desired reaction but a number of other properties need to be addressed.

A single critical number is the cost of the catalyst material. Palladium, the catalyst under consideration, is a precious metal and its price is certainly not negligible for large scale applications.

Changing the PES towards one reaction may also enhance the rate of other chemical reaction, which often cause undesired products. Therefore one aims for a catalyst with a high selectivity, meaning it predominately enhances a desired chemical reaction.

The case that a catalysts is *not* consumed by a chemical reaction, is only an ideal case. Many catalysts have a limited lifetime due to corrosion, sintering [13, 14], or coking [15] or other forms of poisoning [16, 17] to name a few effects. After being deactivated the catalyst needs to be replaced.

In a comprehensive methodology aiming for rational design of catalysts all these aspects need to be addressed. In view of the complexity of reactivity alone, we will focus on this aspect from now on.

1.3 CO OXIDATION ON PALLADIUM

The current study will focus on Palladium as a catalyst for CO oxidation. It is one of several materials commercially used for three-way catalysts. [16–18] The question whether surface oxides hinder or assist surface reactions is important to answer to set the course for further investigations. With the current work I cannot answer this question, but hopefully open a path to this answer.

The Palladium (100) surface under various oxygen pressures has been investigated by several experimental groups. [19–22] The structure was elucidated from a theoretical point of view by Todorova *et al.* [23–26]. Rogal *et al.* found that a surface oxide is stable for conditions very close to industrial use. [27–29]. Rogal's dissertation[1] has been the corner stone of this study.

Experimental investigations on the reactivity of Palladium have been performed mainly in the groups of Goodman and Frenken. [30–33] Presently there is an unresolved debate whether the oxidized or the metallic Palladium is more reactive towards CO oxidation. [34, 35]

1 http://www.diss.fu-berlin.de/2006/535/

Previous studies indicate that Palladium is highly reactive at least very close to this phase boundary between oxide and metallic Palladium. Therefore a profound knowledge of the reconstruction mechanism and the resulting reaction kinetics in this regime are crucial to understand the importance of this oxide.

Phase transitions are particularly interesting since experience shows that catalysts are most reactive at conditions where domination of one surface species changes to another. [36] Ziff *et al.* coined this phenomenon kinetic phase transition. [37]

The fact that Palladium undergoes a non-trivial surface reconstruction, when an oxide is formed adds an intrinsic complexity to the system's behavior and inhibits a straightforward application of atomistic modeling techniques such as lattice kMC (section 2.3.3). On the other hand to deploy off-lattice kMC currently requires further development for our problem (section 2.3.2). The present study therefore endeavors the route to incorporate more than one lattice in a lattice kMC simulation, namely Palladium (100) and the $\left(\sqrt{5} \times \sqrt{5}\right) R27^\circ$ Palladium oxide reconstruction—hence the name multi-lattice kinetic Monte Carlo.

1.4 OUTLINE

The following sections are organized as follows. First I will motivate why we use kinetic Monte Carlo simulations and explain the kMC algorithm. Afterward an outline of how to do multi-lattice kinetic Monte Carlo simulations is given. This allows us to develop a new model incorporating sites from both lattices. Then I will present first results obtained from applying the method to CO oxidation on Pd(100). Finally, results are critically discussed and an outlook for an improvement and expansion of the model is given. A detailed description of the developed model as well as an outline of the developed simulation framework is given in the Appendix.

2 METHODS

After having developed a first picture how a chemical reaction can be accelerated in the presence of a catalyst in principle, we will establish the state-of-the-art of methods to quantitatively predict the evolution of such a system in practice.

We will start very broadly introducing approaches for a quantitative modeling of condensed matter with a bias towards heterogeneous catalysis. We will proceed from small to large scales, inevitably encountering kinetic Monte Carlo. Since an extension of kinetic Monte Carlo is at the center of this study, special emphasis is placed here.

A MULTISCALE PROBLEM A main difficulty is the inherent multiscale character of the problem. At the lowest level one needs to draw on quantum mechanics to understand how chemical bonds are formed and broken to explain the elementary steps. A working catalyst is characterized by a multitude of such elementary steps that occur just in the right order and ratio. In the following I will illustrate that several scales on the temporal as well as on the spatial axis need to be considered for a comprehensive description.

LEVEL OF DETAIL Before delving into various approaches we ought to have a measure for the suitability of a method. It is a truism that at the end of a theoretical calculation one would like (a) to have a result and (b) it should be possible to validate this result by experiment. For the first part the method needs to be applicable (by pencil or computer processors) within a reasonable time (1 year, 3 years, ...) and for the latter we need to include as many details from the considered system as necessary. That means for a successful method the level of detail needs to be just right.

Starting from quantum mechanics the total number of degrees of freedom of a few hundreds of atoms is truly humiliating. The only way of treating such a system is by integrating out or better contracting a properly chosen part of detailedness.

TURN-OVER FREQUENCY The observable of main interest here is ultimately the number of reactants that are converted to desired or undesired products per unit area and unit time, which has been coined turn-over frequency (TOF). The input variables most commonly used in experiment are the temperature T and partial gas pressures of reactants $\{p_i\}$. One could say one overall goal of a theory of heterogeneous catalysis is to be able to find $\mathrm{TOF}_c\left(T, \{p_i\}\right)$ for an arbitrary catalyst c without resorting to experimental parameters.

STEADY STATE An important concept here is a more generalized version of thermodynamic equilibrium called steady-state. Species in a gas phase, which we would like to react are reactants or educts. Gas phase species that are formed are said to be products. Particles that are adsorbed on a surface are said to be in an intermediate state or reaction intermediates. In thermodynamic equilibrium the concentration

of each of those is independent of time which would mean that catalytic conversion no longer takes place. However since we would like to describe the very conversion of reactant to products in a catalytic process (note at equilibrium TOF $\equiv 0$) we need to relax this constraint. A unambiguous system-independent definition of a steady state is non-trivial because sometimes large spatiotemporal fluctuations are observed under what is considered steady-state conditions. As a simplified definition we resort to find the TOF $(T, \{p_i\})$ at a *steady-state*, *i.e.* when the concentration of all reaction intermediates $\{c_i^{interm.}\}$ is nearly constant: $\partial_t c_i^{interm.} \approx 0 \forall i$.

2.1 CONTINUOUS TRAJECTORY APPROACHES

On an atomic or molecular level several approaches have been developed that aim for a realistic description of a continuous trajectory of the system in phase space. Such approaches are extremely inefficient for rare-event dynamics. [9]

Starting very naively one could try to solve the Schrödinger equation for all substrate and adsorbate nuclei and electrons and propagate the solution forward in time. Obviously this is quite far from a practical approach.[1] A much more contracted level of description and closer to a classical description would be to construct potentials for the movement of nuclei and simulate the system by integrating the Newton equation of motion for those nuclei. This approach is known as Molecular Dynamics (MD) [38] but it is still impractical for the problem at hand. The time step necessary for an accurate integration is dictated by the timescale of atomic vibrations $\left(\sim 10^{-13}\text{s}\right)$ while typical barrier crossings may take place on the order of every $\sim 10^{-7}$s—and we are only interested in the crossings! That means one would on average need to simulate one million vibrations before observing any transition. Simulating enough crossings to obtain a reliable statistics is certainly out of reach for today's fastest computers and also not very economical.

A system that evolves in such a way is said to obey rare-event dynamics. One should not get confused into thinking that any event is rare. Atoms vibrate quite fast, only the events we consider crucial are extremely rare in comparison. This dismisses any approach that describes a continuous trajectory. Evidently a more contracted description is necessary that captures transitions most efficiently. Such a method is based on the master equation.

2.2 THE MASTER EQUATION

Consider a system that is in a state i with a probability p_i. This state could for instance be a set of coordinates, occupied energy levels, or a configuration of spins. Let $k_{ji}\mathrm{d}t$ denote the probability, that the system transitions from i to j in an infinitesimal time interval $\mathrm{d}t$. Then the equation of motion for p_i can be written as

1 One can easily estimate that in order to accurately represent the full wave function of a one multi-electron atom several tons of DVDs are needed. A second problem is that the time step needed to accurately propagate the electronic wave function leads to a very inefficient evaluation of the dynamics of the nuclei.

$$\frac{\mathrm{d}p_i}{\mathrm{d}t} = \sum_j -k_{ji}p_i + k_{ij}p_j,$$

which is known as the Master equation. It is important to note that one assumed that k_{ji} only depends on the states i and j and not on which state the system has been previously in.

The previous assumption is known as *Markov* approximation. [39] This is arguably a good assumption if the system spends much more time in one state than the time it takes to transition between states. One can imagine that during this stay the system somehow forgets where it came from.

The main advantage of a master equation based approach is that it allows to contract the full trajectory between two transitions to a single event and generate only a state-to-state trajectory. We can think of one state in the sense of the master equation as one configuration of particles on adsorption sites and only need to find the transition probabilities between states. That means, the only information we keep from a high dimensional PES is a single number representing how often elementary steps occur on average (how this can be done in practice is described in section 2.5).

Unfortunately solving the full master equation analytically is still impossible in practice. If we chose to represent the state of a system by a grid of integers and with at least two surface species (a minimum for Langmuir-Hinshelwood type reactions), which would mean 3 possible values (*A*, *B*, *empty*) for each grid point and a linear size L there would be 3^{L^2} different surface states. Worse, the matrix holding all transition rates would have a size of $3^{L^2} \times 3^{L^2} = 3^{2L^2}$entries. Even a moderate lattice with $L = 10$ we would end with roughly 10^{95} numbers! Experience shows that a linear grid size of 10 may be insufficient to faithfully represent many surface phenomena and finite-size effects such as fluctuations become increasingly large. Nevertheless, this equation can be solved approximately using the numerical method of kinetic Monte Carlo (kMC).

2.3 KINETIC MONTE CARLO METHODS

KMC is a numeric method to approximate the solution of the master equation. From the perspective of the master equation one chooses rate constants $\{k_{ij}\}$, which are estimates for the transition rates between states $\{i\}$. Yet, instead of solving the master equation to obtain p_i analytically, we generate an ensemble of trajectories and extract desired quantities by averaging over trajectories.

The steps can be described as follows

Algorithm 1: Basic kMC

Fix rate constants k_{ij},
initial state x_i, and initial time t
while $t < t_{max}$ **do**
Draw random numbers $R_1, R_2 \in]0,1]$ ①
Find l such that $\sum_{j=1}^{l} k_{ij} < k_{i,tot} R_1 \leq \sum_{j=1}^{l+1} k_{ij}$ ②
Change state $x_i \to x_l$ ③
Increment time $t \to t - \frac{\ln(R_2)}{k_{i,tot}}$ ④
end

2.3.1 *Justification of the Algorithm*

Next, one should understand why this simulates a physical process. The Markov approximation mentioned above implies several things: not only does it mean one can determine the next process from the current state. It also implies that all processes happen independently of one another because any memory of the system is erased after each step. Another great simplification is that rates simply add to a total rate, which is sometimes referred to as Matthiessen's rule, *viz.* the rate with which *any* process occurs is simply $k_{tot} = \sum_i k_i$.

First, one can show that the probability that n such processes occur in a time interval t is given by the Poisson distribution [40]

$$P(n,t) = \frac{e^{-k_{tot}t} (k_{tot}t)^n}{n!}.$$

The waiting time or escape time t_w between two such processes is characterized by the probability that *zero* such processes have occurred

$$P(0,t_w) = e^{-k_{tot}t_w}, \tag{2.1}$$

which, as expected, leads to an average waiting time of

$$\langle t_w \rangle = \frac{\int_0^\infty \mathrm{d}t_w \, t_w e^{-k_{tot}t_w}}{\int_0^\infty \mathrm{d}t_w \, e^{-k_{tot}t_w}} = \frac{1}{k_{tot}}.$$

Therefore at every step, we need to advance the time by a random number that is distributed according to (2.1). One can obtain such a random number from a uniformly distributed random number $R_2 \in]0,1]$ via $-\ln(R_2)/k_{tot}$, [41] thus ④.

Second, we need to select the next process. The next process occurs randomly but if we did this a very large number of times for the same state the number of times each process is chosen should be proportional to its rate constant. Experimentally one could achieve this by randomly sprinkling sand over an arrangement of buckets, where the size of the bucket is proportional to the rate constant and count each hit by a grain of sand in a bucket as one executed process. Computationally the same is achieved by ② and ③.

Altogether we need two random numbers, thus ①.

The ideas of kMC have been developed in different areas apparently independent of another with differing names and formulations.

The earliest formulation is often accredited to Bortz *et al.* [42] (here called the n-fold way or BKL-method), while Gillespie [43] is credited frequently, too (here called Gillespie method or dynamical Monte Carlo, DMC). The latter is more often referred to in biological applications. Fichthorn and Weinberg demonstrated that a rigorous connection between simulated kMC time and physical time exists. [44] This gives kMC a key advantage over equilibrium Monte Carlo methods (Metropolis, etc.) for our problem, since the latter is not suitable for simulating non-equilibrium kinetics.

A seminal paper by Ziff *et al.* [45, 46] did not use rejection-free kMC but successfully illustrated the advantage of treating surface kinetics atomistically. They demonstrated in particular the importance of fluctuations as well as the response to dynamical input, which is generally not captured by mean-field methods.

In the meantime a lot of progress has been made in improving the efficiency of the underlying algorithms. Crucial are a set of ideas, which allow the CPU time needed per kMC step to be independent of the number of sites, O(1). Note that doubling the system size still bisects the simulated time. The significance of local updating algorithms is explained in the review article by Vlachos *et al.* [47], while an essential ingredient[2] is how to update the book-keeping database as described by Reese *et al.* [48] based on a paper by Nicholson [49].

Pedagogical and detailed introductions to the kMC method in the context of surface kinetics are given by Jansen [50], Reuter [9], and Voter [51].

2.3.2 *Off-lattice KMC Modeling*

KMC as an approximate solver of the master equation is not limited to a certain geometry or number of dimensions. The task to set up a catalog of all relevant states and transitions for an arbitrary real system is, nevertheless, a daunting one. Currently several approaches that aim to construct transition states and rate constants during the simulation (on-the-fly) only starting from a stable initial structure are under active development. Such approaches are coined adaptive kMC by Henkelman *et al.* [52], self-learning kMC by Trushin *et al.* [53, 54], or kinetic Activation Relaxation Technique by Mousseau *et al.* [55].

Let us gather the main challenges a general kMC approach faces in a system of N particles in 3 dimensions. Given a stable initial geometry (which is characterized by a local minimum of the $3N$ dimensional PES function) one needs to find all relevant escape paths; that means one needs to find all saddle points of the PES below a certain threshold energy (*e.g.* $\sim 20 k_B T$), that are connected to the initial geometry. Higher lying saddle-points can usually be ignored since they are expected to occur less often by 9 orders of magnitude and contribute little to k_{tot} in ④. This task alone is particularly daunting especially if no further restriction can be made on the degrees of freedom. Formally a saddle point can be characterized by a Hessian matrix of the PES, which has exactly one negative eigenvalue. Yet, since calculating and diagonalizing Hessians is computationally not always viable, methods such as dimer search [56] and activation relaxation technique (ART) [57, 58] have been developed that only need first derivatives.

2 I would like to thank S. Matera for pointing this out.

Second, for heterogeneous catalysts we are often dealing with crystalline structures. If the system is not dominated by defects, one expects a large number of degenerate low lying transition paths, *e.g.* because each atom can perform a very similar diffusion hop from a number of equivalent sites in the crystal. This means in the general case the degeneracy scales at least linearly with N. This raises the following question: If I found a number of saddle points already, when can I stop searching? Henkelman *et al.* put forward a somewhat heuristic scheme that introduces a level of confidence, that all relevant saddle points have been found after a certain number of searches. [52] Mousseau uses a fixed number of searches per atom that he considers extensive. [59]

Lastly, in order to actually harvest the efficiency of kMC, one needs to reuse previously found transitions. Therefore some pattern recognition scheme needs to be devised to identify local structures (the size of such a structure is of course defined by the interaction lengths in the system) and reapply previously calculated transition paths and rate constants. Henkelman suggests to iteratively replace particles that moved by more than a certain threshold distance (0.2Å) in the last step, by the corresponding particle of all known previously calculated saddle points. [52] While practical this would need some modification in an open system such as a catalyst. Mousseau constructs a graph, a concept from graph theory in computer science, representing a certain environment around each atom to recognize previously known local structures. [55] The prescription of how to construct a graph of course needs to be adapted to the system at hand.

In summary a general off-lattice kMC scheme is, yet, a very complex task that contains several open technical challenges. One can expect several forthcoming schemes in the next few years. It would be an interesting problem to define graph construction rules together with saddle point search criteria that recover the process list of a known lattice based kMC model such as the one for CO oxidation on RuO_2 by Reuter *et al.* [60].

2.3.3 *Lattice KMC Modeling*

On the other hand in a first approximation all the challenges above are met within a lattice approximation. In section 1.2.1 we noted that on heterogeneous catalysts particles adsorb on certain spots on the surface called adsorption sites. In the following application we will approximate the space accessible to particles by a lattice of those adsorption sites.

Within the lattice approximation the dimensionality of the PES is drastically reduced since we only consider a discretized subspace of the full configuration space. Second, the number of needed saddle-point searches is comparably low, since we only consider initial and final states that can be represented on the lattice. Furthermore the number of final states for each initial state can be reduced by arguments of chemical intuition. Lastly, the reuse of known transition paths becomes trivial since recognition of local structures reduces to a few *if*-statements on an array representing the lattice.

If the system of interest has a lattice symmetry we only have to calculate rates for processes between inequivalent sites. This is a great advantage if the calculation of each rate is computationally expensive.

In effect we often only need to consider (and implement) a few dozen of inequivalent processes even though the simulated system may contain hundreds or more sites. It is the number of inequivalent sites and species that determines the models complexity. The set of inequivalent processes is called *process list*.

AB INITIO MODELING The fact that in simpler systems on a lattice one only needs $\sim 10^2$ different rate constants inspired a very ambitious approach to obtain the underlying barriers solely from first-principles methods such as DFT. How to link energy barriers to rate constants is explained in section 2.5. Even though the calculation of each energy barrier is computationally quite expensive it only has to be done once per elementary step and kMC allows to predict rates due to the interplay of elementary steps for a whole range of thermodynamic conditions entirely based on *ab initio* data. Reuter *et al.* successfully used barriers from electronic structure calculations of RuO_2 to construct a kMC model which demonstrates that catalytic activity can be predicted quantitatively from first-principles. [60–62]

2.3.4 *Critique of Lattice KMC*

A lattice kMC model ultimately hinges on a well guessed process list. The source of these guesses is usually referred to as *chemical intuition*. Surface science researchers commonly sharpen their chemical intuition with a range of evidences such as structures from DFT calculations, LEED[3] experiments, STM[4] pictures, reactivity measurements, and TPD[5] spectra. Nevertheless, the application of this chemical intuition to construct microscopic models remains a highly heuristic and in many ways unsatisfying art for a theorist who would like to claim predictive power independent of experimental input.

Even the phase space of less than a dozen atoms quickly evades our imagination. Therefore any kMC model is prone to overlook mechanisms, which only experiments can elucidate. Examples are a diffusion mechanism by switching with substrate atoms instead of hopping [63, 64] or more recently unexpected surface reconstructions on Platinum with high CO coverage [65].

Sensitivity-analysis may help in finding programming errors and can be used to assess the error propagation from electronic structure calculations. [66] However within kMC one can not assess the gravity of a neglected process itself.

On the other hand kMC can be regarded an excellent test bed for ideas about microscopic processes. To the best of my knowledge it is the only method that is able to capture events on the picoseconds scale and cover simulation times up to seconds while not making assumptions about spatial distributions in the system other than the lattice approximation. Even away from thermodynamic equilibrium it is able to retain detailed microscopic information and a direct measure of the time evolution.

Apart from the numerical results the method produces, it proved to be a practical tool for fundamental understanding even before any simulation is carried out. When constructing reaction pathways one is

3 LEED stands for Low Energy Electron Diffraction.
4 STM stands for Scanning Tunneling Microscope.
5 TPD stands for Temperature Programmed Desorption.

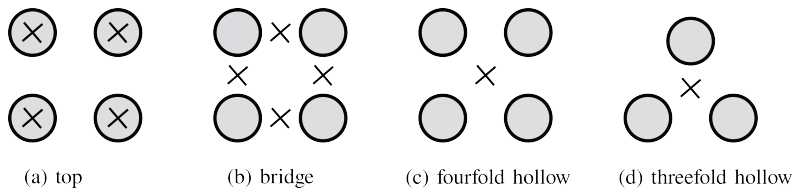

Figure 3: Schematic representation of high-symmetry adsorption sites

forced to think about various steps in a detailed and spatially resolved way. Thereby formerly obscure phenomena, in particular the interplay of different processes, often can be readily explained. [61]

2.3.5 *KMC Jargon*

When one actually uses or develops kMC models (*e.g.* in the following chapter), one typically uses a certain amount of domain specific language better known as terminology or jargon. This jargon typically creates unnecessary barriers to outsiders, so an explanation shall be given.

One categorizes surface adsorption sites into three kinds with respect to the underlying substrate atoms. Even though this has nothing to do with kMC directly, it is frequently encountered first when motivating a kMC process list. If an atom or molecule binds directly over an atom it is said to bind *on top*. If an atom or molecule binds midway over two atoms it is said to bind *on bridge*. If an atom or molecule binds over the center of three or more atoms it is said to bind *on hollow*. Sometimes one also differentiates *threefold hollow* and *fourfold hollow.* Of course one should also indicate which surface is discussed if ambiguous. See also figure 3.

The words *process* and *reaction* are often used interchangeably. In this work anything that happens exactly once during a kMC step is said to be a process. Reaction is reserved for the chemical reaction itself, *i.e.* here $CO+\frac{1}{2}O_2 \rightarrow CO_2$.

Rate constant means how many *times per second* a process occurs that is possible due to the local configuration, whereas *rate* means how often a process actually occurs in a system.

2.4 MEAN-FIELD APPROACHES

An even more contracted description is accomplished by mean-field approximations which is also a popular tool to predict a catalysts reactivity. Mean-field approaches such as rate equations describe a heterogeneous catalyst in terms of reaction intermediate concentrations. A set of coupled differential equations is set up using rate constants for elementary steps, which can be solved numerically to calculate steady-state concentrations and reaction frequencies. Rate constants can be calculated from first principles and one can obtain a rough estimate (often an upper estimate) for the reactivity. However the method typically fails quantitatively and often also qualitatively because it oversimplifies the system: a distribution of adatoms of one species on the surface is represented by a single number! If we calculated a low reaction barrier for certain local configuration of atoms, but this situation occurs very rarely because binding energies favor a different local configura-

tion, this barrier only has little meaning. [67] Another example is if attractive lateral interaction promotes formation of islands and species may only react at the interfaces between islands. This can reduce the number of reactions by orders of magnitude. Simply speaking: as soon as the system deviates from a randomly mixed distribution, mean-field approaches can introduce serious errors.

2.5 RATE CONSTANTS

Transition-state theory

As mentioned above a second important ingredient to kMC are the rate constants. Transition-state theory is a set of concepts and approximations that is commonly used to calculate rate constants based on barriers obtained from electronic structure calculations. Hänggi *et al.* reviewed various aspects of transition-state theory including quantum mechanical effects due to tunneling. [68] Detailed discussions can be found in text books. [69, 70] Despite the myriad of studies on this topic, open questions remain. Even if one constrains the focus to simple or harmonic transition state theory I could not find a satisfying derivation of the formula, what Hänggi refers to as *flux-over-population* method. To understand the formulae used in the simulation I present an elementary derivation following Chandler [71].

The problem of calculating transition rates constants can be formulated as the question of how long it takes for a particle to escape from one strongly binding basin to another one.

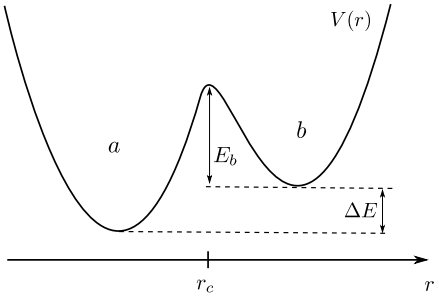

Figure 4: Double-well potential with two metastable states.

Suppose we have a 1-dimensional double-well potential with basins a, b and a dividing energy barrier E_b at r_c, and the temperature is such, that $k_B T \ll E_b$. Suppose in this potential there are N independent particles with trajectories $q_i(t)$ with $i = 1, \ldots, N$. Then for any time t the number of particles in each basin is

$$\begin{aligned} N_a(t) &= \sum_{i=1}^{N} \Theta(r_c - q_i(t)) \\ N_b(t) &= \sum_{i=1}^{N} \Theta(q_i(t) - r_c) = N - N_a(t) \end{aligned}$$

where Θ is the Heaviside function

$$\Theta(x) = \begin{cases} 1 & x > 0 \\ 0 & x < 0. \end{cases}$$

Close to thermodynamic equilibrium we assume a linear dependence on some rate constants ($k_{\rightarrow}, k_{\leftarrow} > 0$):

$$\dot{N}_a(t) = -k_{\rightarrow} N_a(t) + k_{\leftarrow} N_b(t) \tag{2.2}$$
$$\dot{N}_b(t) = -k_{\leftarrow} N_b(t) + k_{\rightarrow} N_a(t) \tag{2.3}$$

where $k_{\rightarrow}$ is the rate constant of particles moving from a to b and $k_{\leftarrow}$ is the rate constant of particles moving from b to a. These equations are in fact purely empirical and our transition rates would have to be modified if experimentalists reported a different behavior.

In equilibrium the left-hand side of these two equations must vanish and one can rearrange to

$$\frac{k_{\rightarrow}}{k_{\leftarrow}} = \frac{\langle N_b \rangle}{\langle N_a \rangle}$$

which is better known as the *detailed balanced criterion* and $\langle \dots \rangle$ indicates the thermodynamic average. In thermal equilibrium this means, if the energies of basins a and b are separated by $\Delta E = E_b - E_a$, we know that $\langle N_a^{-1} \rangle e^{-\beta E_a} = \left\langle N_b^{-1} \right\rangle e^{-\beta E_b}$ (where $\beta = \frac{1}{k_B T}$) or

$$\frac{k_{\rightarrow}}{k_{\leftarrow}} = e^{-\beta \Delta E}.$$

If we disturb the system slightly, *i.e.* move $M \ll N_a, N_b$ particles from a to b, we can solve (2.2), (2.3) with the following Ansatz:

$$N_a(t) = -Me^{-\kappa t} + \langle N_a \rangle$$
$$N_b(t) = Me^{-\kappa t} + \langle N_b \rangle$$

which means

$$\dot{N}_a(t) = \kappa M e^{-\kappa t}$$
$$\dot{N}_b(t) = -\kappa M e^{-\kappa t}.$$

Plugging this into say (2.3), we get

$$\kappa M e^{-\kappa t} = -k_{\rightarrow} \left(-Me^{-\kappa t} + \langle N_a \rangle \right) + k_{\leftarrow} \left(Me^{-\kappa t} + \langle N_b \rangle \right),$$

which we can rearrange to

$$Me^{-\kappa t} \left(\kappa - (k_{\rightarrow} + k_{\leftarrow}) \right) = -k_{\rightarrow} \langle N_a \rangle + k_{\leftarrow} \langle N_b \rangle .$$

According to detailed-balance the right-hand side must vanish, and since $Me^{-\kappa t} \neq 0$ follows

$$\kappa = k_{\rightarrow} + k_{\leftarrow}.$$

and

$$\frac{N_a(t) - \langle N_a \rangle}{N_a(0) - \langle N_a \rangle} = e^{-(k_{\rightarrow} + k_{\leftarrow})t}.$$

This result can be coupled to microscopic dynamics with the observation that for a small perturbation the effect on a dynamical variable $A(t)$ decays just like the time-correlation of fluctuations of that variable or more mathematically put

$$\frac{\bar{A}(t) - \langle A \rangle}{\bar{A}(0) - \langle A \rangle} = \frac{\langle \delta A(t)\, \delta A(0) \rangle}{\langle (\delta A(0))^2 \rangle}$$

where $\bar{A}$ means that A is just weakly perturbed and $\delta A(t) = A(t) - \langle A \rangle$.

To derive this statement suppose our unperturbed system is given by the Hamiltonian H_0 and a weak perturbing field f couples linearly to $A(t)$ at $t = 0$ so that we have a perturbed system

$$H = H_0 - fA(0) = H + V.$$

The thermodynamic average of $\bar{A}(t)$ is then

$$\left\langle \bar{A}(t) \right\rangle = \frac{\mathrm{Tr}\left\{ A(t)\, e^{-\beta(H_0+V)} \right\}}{\mathrm{Tr}\left\{ e^{-\beta(H_0+V)} \right\}}.$$

If we can assume $V \ll H_0$ and $[V, H_0] \approx 0$, which is of course true in the classical case, we can expand

$$\begin{aligned}
\left\langle \bar{A}(t) \right\rangle &= \frac{\mathrm{Tr}\left\{ A(t)\, e^{-\beta H_0}(1 - \beta V) \right\}}{\mathrm{Tr}\left\{ e^{-\beta H_0}(1 - \beta V) \right\}} + O\left(V^2\right) \\
&= \frac{\mathrm{Tr}\left\{ A(t)\, e^{-\beta H_0} \right\} - \beta \mathrm{Tr}\left\{ A(t)\, V e^{-\beta H_0} \right\}}{\mathrm{Tr}\left\{ e^{-\beta H_0} \right\} - \beta \mathrm{Tr}\left\{ V e^{-\beta H_0} \right\}} + O\left(V^2\right) \\
&= \frac{\mathrm{Tr}\left\{ A(t)\, e^{-\beta H_0} \right\}}{\mathrm{Tr}\left\{ e^{-\beta H_0} \right\}(1 - \beta \langle V \rangle)} - \beta \frac{\mathrm{Tr}\left\{ A(t)\, V e^{-\beta H_0} \right\}}{\mathrm{Tr}\left\{ e^{-\beta H_0} \right\}(1 - \beta \langle V \rangle)} + O\left(V^2\right) \\
&= \frac{\langle A(t) \rangle - \beta \langle A(t)\, V \rangle}{1 - \beta \langle V \rangle} + O\left(V^2\right) \\
&= (\langle A(t) \rangle - \beta \langle A(t)\, V \rangle)(1 + \beta \langle V \rangle) + O\left(V^2\right) \\
&= \langle A(t) \rangle - \beta \langle VA(t) \rangle + \beta \langle A(t) \rangle \langle V \rangle + O\left(V^2\right).
\end{aligned}$$

If we neglect terms of order higher than linear in V and plug in $V = -fA(0)$ we get

$$\left\langle \bar{A}(t) \right\rangle = \langle A(t) \rangle + \beta f \left(\langle A(0)\, A(t) \rangle - \langle A(t) \rangle \langle A(0) \rangle \right)$$

or

$$\bar{A}(t) - \langle A \rangle = \beta f \left(\langle A(0)\, A(t) \rangle - \langle A(t) \rangle \langle A(0) \rangle \right), \tag{2.4}$$

which means in particular at $t = 0$

$$\bar{A}(0) - \langle A \rangle = \beta f \left(\left\langle A^2(0) \right\rangle - \langle A(0) \rangle^2 \right). \tag{2.5}$$

Combining (2.4) and (2.5) yields:

$$\begin{aligned}\frac{\bar{A}(t)-\langle A\rangle}{\bar{A}(0)-\langle A\rangle} &= \frac{\langle A(0)A(t)\rangle-\langle A(0)\rangle\langle A(t)\rangle}{\langle A(0)A(0)\rangle-\langle A(0)\rangle\langle A(0)\rangle}\\ &= \frac{\langle \delta A(t)\,\delta A(0)\rangle}{\langle \delta A(0)^2\rangle}.\end{aligned}$$

This remarkable result is known as the *Onsager regression hypothesis* and allows us to link the decay of the system's perturbation to fluctuations of microscopic trajectories.

$$e^{-t(k_\rightarrow+k_\leftarrow)} = \frac{\langle \delta N_a(t)\,\delta N_a(0)\rangle}{\langle (\delta N_a)^2\rangle}.$$

In a dilute system, we can assume that trajectories do not affect each other and instead of calculating averages over multiple trajectories we can treat them as independent and approximate

$$\begin{aligned}\langle N_a(t)\rangle &\approx N\langle\Theta(r_c-q(t))\rangle\\ \langle N_b(t)\rangle &\approx N\langle\Theta(q(t)-r_c)\rangle\end{aligned}$$

and

$$\begin{aligned}e^{-(k_\rightarrow+k_\leftarrow)t} &= \frac{\langle \delta\Theta(r_c-q(t))\,\delta\Theta(r_c-q(0))\rangle}{\left\langle(\delta\Theta(q-r_c))^2\right\rangle}\\ &= \frac{\langle\Theta(r_c-q(t))\,\Theta(r_c-q(0))\rangle-\langle\Theta(r_c-q)^2\rangle}{\left\langle(\delta\Theta(q-r_c))^2\right\rangle}\end{aligned} \tag{2.6}$$

If we introduce the abbreviations $n_a=\langle N_a\rangle/N$ and $n_b=\langle N_b\rangle/N$ we can simplify

$$\begin{aligned}\langle(\delta\Theta(q-r_c))^2\rangle &= \langle(\Theta(r_c-q)-n_a)(\Theta(r_c-q)-n_a)\rangle\\ &= \underbrace{\langle\Theta^2(r_c-q)\rangle}_{\equiv\Theta(r_c-q)}-\langle\Theta(r_c-q)\,n_a\rangle-\langle n_a\Theta(r_c-q)\rangle+n_a^2\\ &= n_a-n_a^2=n_a(1-n_a)\\ &= n_an_b\end{aligned}$$

since $n_a+n_b=1$ and if we take the time-derivative of (2.6) we get

$$-(k_\rightarrow+k_\leftarrow)\,e^{-(k_\rightarrow+k_\leftarrow)t} = \frac{\langle\dot\Theta(r_c-q(t))\,\Theta(r_c-q(0))\rangle}{n_an_b}. \tag{2.7}$$

The enumerator on the right-hand side of (2.7) can be simplified by exploiting the ergodic hypothesis and

$$\begin{aligned}\langle\dot\Theta(r_c-q(t))\,\Theta(r_c-q(0))\rangle &= -\langle\dot\Theta(r_c-q(-t))\,\Theta(r_c-q(0))\rangle\\ &= -\langle\dot\Theta(r_c-q(0))\,\Theta(r_c-q(t))\rangle\\ &= -\langle\delta(r_c-q(0))\,\dot q(0)\,\Theta(r_c-q(t))\rangle\\ &= -\langle\delta(r_c-q(0))\,\dot q(0)\,[1-\Theta(q(t)-r_c)]\rangle\\ &= -\underbrace{\langle\delta(r_c-q(0))\,\dot q(0)\rangle}_{=0\text{ due to symmetry}}\\ &\quad+\langle\delta(r_c-q(0))\,\dot q(0)\,\Theta(q(t)-r_c)\rangle\end{aligned}$$

and lastly since:

$$\begin{aligned} k_{\rightarrow} + k_{\leftarrow} &= k_{\rightarrow}\left(1 + \frac{k_{\leftarrow}}{k_{\rightarrow}}\right) = k_{\rightarrow}\left(1 + \frac{n_a}{n_b}\right) = k_{\rightarrow}\left(\frac{n_a + n_b}{n_b}\right) \\ \Rightarrow k_{\rightarrow} &= n_b\left(k_{\rightarrow} + k_{\leftarrow}\right) \end{aligned}$$

we get

$$k_{\rightarrow}(t)\, e^{-(k_{\rightarrow}+k_{\leftarrow})t} = \frac{\langle \delta(r_c - q(0))\, \dot{q}(0)\, \Theta(q(t) - r_c)\rangle}{n_a}$$

For the regime of interest it seems justified to consider a time scale Δt that is much longer than the movement of single particles $\tau_{\text{part.}}$ but much shorter than $(k_{\rightarrow} + k_{\leftarrow})^{-1}$:

$$\tau_{\text{part}} \ll \Delta t \ll (k_{\rightarrow} + k_{\leftarrow})^{-1}$$

which means we have coarse-grained over several single-particle movements so that (2.2), (2.3) are valid but still

$$e^{-(k_{\rightarrow}+k_{\leftarrow})\Delta t} \approx 1$$

and

$$k_{\rightarrow}(t) = \frac{\langle \delta(r_c - q(0))\, \dot{q}(0)\, \Theta(q(t) - r_c)\rangle}{n_a}. \tag{2.8}$$

This equation can be simplified further in the limit $t \to 0^+$: in (2.8) only those trajectories are accounted for, that have $q = r_c$ for $t = 0$ and at $t = 0^+$ they have to be at r_c or to the right of r_c due to the factor $\Theta(q(t = 0^+) - r_c)$. In short the velocity at $t = 0$ has to be positive so we can also write

$$\left\langle \delta(r_c - q(0))\, \dot{q}(0)\, \Theta\left(q\left(0^+\right) - r_c\right)\right\rangle = \langle \delta(r_c - q(0))\, \dot{q}(0)\, \Theta(\dot{q}(0))\rangle .$$

If we assume that even at later times no particles recross the barrier, this is called the transition state approximation and we get

$$k_{\rightarrow}^{TST} = \frac{\langle \delta(r_c - q)\, \dot{q}(0)\, \Theta(\dot{q})\rangle}{n_a}.$$

Note that $k_{\rightarrow}^{TST}$ is always an upper boundary for $k_{\rightarrow}$ since it excludes those trajectories that recross the barrier before thermalizing in basin b.

We shall now evaluate this expression for a common application:

$$H = \frac{p^2}{2m} + V(q)$$

where V is a potential that still has to be specified. We can write down the expectation values as usual

$$\begin{aligned} k_{\rightarrow}^{TST} &= \frac{2\pi\hbar}{2\pi\hbar}\frac{\int \mathrm{d}q\mathrm{d}p\,\delta\left(r_c-q\right)\frac{p}{m}\Theta\left(p\right)e^{-\beta H}}{\int \mathrm{d}q\mathrm{d}p\,\Theta\left(r_c-q\right)e^{-\beta H}} \\ &= \frac{Z_0^{-1}}{2\pi\hbar}e^{-\beta V(r_c)}\int_0^\infty \mathrm{d}p\,\frac{p}{m}e^{-\beta p^2/2m} \\ &= \frac{Z_0^{-1}}{2\pi\hbar}e^{-\beta V(r_c)}\int_0^\infty \mathrm{d}p\,\frac{-2m}{2\beta m}\frac{\partial}{\partial p}e^{-\beta p^2/2m} \\ &= \frac{Z_0^{-1}}{2\pi\hbar}e^{-\beta V(r_c)}\left[-e^{-\beta p^2/2m}\right]_{p=0}^{\infty} \\ &= \frac{Z_0^{-1}}{2\pi\hbar\beta}e^{-\beta V(r_c)} \end{aligned}$$

with

$$\begin{aligned} Z_0 &= \frac{1}{2\pi\hbar}\int \mathrm{d}q\mathrm{d}p\,\Theta\left(r_c-q\right)e^{-\beta\left(\frac{p^2}{2m}+V(q)\right)} \\ &= \sqrt{\frac{2\pi m}{\beta}}\int\frac{\mathrm{d}q}{2\pi\hbar}\,\Theta\left(r_c-q\right)e^{-\beta V(q)} \\ &= \sqrt{\frac{m}{2\pi\beta\hbar^2}}\int_{-\infty}^{r_c}\mathrm{d}q\,e^{-\beta V(q)}. \end{aligned}$$

In the limit of low temperatures one can use the saddle-point trick (also known as method of steepest- descent) [72] to evaluate this integral. The idea is that if $V\left(q\right)$ is not too shallow around its minimum at q_0 and $\beta \gg 1$, the largest contribution comes from the region very close to this minimum. Since we hope that contributions further away from the minimum are very small, we extend the region of integration over the entire space. At the minimum we can expand the potential in a Taylor series

$$\begin{aligned} V\left(q\right) &= V\left(q_0\right)+\left(q-q_0\right)\underbrace{\frac{\partial}{\partial q}V\left(q_0\right)}_{=0}+\frac{1}{2}\left(q-q_0\right)^2\frac{\partial^2 V\left(q_0\right)}{\partial q^2}+\ldots \\ &= V\left(q_0\right)+\frac{1}{2}\left(q-q_0\right)^2 V''\left(q_0\right)+\ldots \end{aligned}$$

and

$$\begin{aligned} Z_0 &\approx \sqrt{\frac{m}{2\pi\beta\hbar^2}}\int_{-\infty}^{\infty}\mathrm{d}q\,e^{-\beta\left(V(q_0)+\frac{1}{2}(q-q_0)^2V''(q_0)\right)} \\ &= \sqrt{\frac{m}{2\pi\beta\hbar^2}}e^{-\beta V(q_0)}\int_{-\infty}^{\infty}\mathrm{d}q\,e^{-\beta\frac{1}{2}(q-q_0)^2V''(q_0)} \\ [q\rightarrow q+q_0] &= \sqrt{\frac{m}{2\pi\beta\hbar^2}}e^{-\beta V(q_0)}\int_{-\infty}^{\infty}\mathrm{d}q\,e^{-\beta\frac{1}{2}q^2V''(q_0)} \\ &= \sqrt{\frac{m}{\beta^2V''\left(q_0\right)\hbar^2}}e^{-\beta V(q_0)} \end{aligned}$$

which means

$$\begin{aligned} k_{\rightarrow}^{TST} &\approx \frac{1}{2\pi\beta\hbar} e^{-\beta V(r_c)} \sqrt{\frac{\beta^2 V''(q_0)\hbar^2}{m}} e^{\beta V(q_0)} \\ &= \frac{1}{2\pi} \sqrt{\frac{V''(q_0)}{m}} e^{-\beta\Delta E} \end{aligned}$$

where $\Delta E = V(r_c) - V(q_0)$.

One important application is a harmonic potential, where the saddle-point approximation coincides with the real potential up to the shifted cut-off. The harmonic potential is given by

$$V(q) = \frac{m}{2}(q - q_0)^2 \omega_0^2 \Rightarrow V''(q_0) = m\omega_0^2,$$

where ω_0 is the angular frequency, and therefore

$$k_{\rightarrow}^{TST} = \frac{\omega_0}{2\pi} e^{-\beta\Delta E}.$$

One could calculate ω_0 with an electronic structure calculation by evaluating the second derivative of the potential energy surface at the minimum but in practice one resorts to a much simpler way: if the potential is harmonic, the energy levels of the particle is a standard problem from quantum mechanics

$$E_n = \hbar\omega_0 \left(n + \frac{1}{2}\right)$$

and assuming that the particle is in its ground state most of the time, we can combine this with the equipartition theorem stating that the average energy per degree of freedom is

$$E = \frac{1}{2\beta} \approx E_0$$

and we get

$$\omega_0 = \frac{1}{\beta\hbar}$$

and finally

$$\boxed{k_{\rightarrow}^{TST} \approx \frac{1}{\beta h} e^{-\beta\Delta E}.}$$

2.6 MULTI-LATTICE KMC

So far we have not discussed the actual lattice used for a lattice kMC simulation. Typical lattice kMC models use a single lattice as known from solid-state physics to represent the configuration of a system. However there are catalysts that display a lattice-like adsorption structure, except that the structure cannot be represented well on a *single* lattice. Instead two or more lattices make up the surface with fractions depending on external parameters. The present example is a monolayer growth of Palladium oxide on Palladium. To be able to represent such a changing geometry, while not giving up the advantages

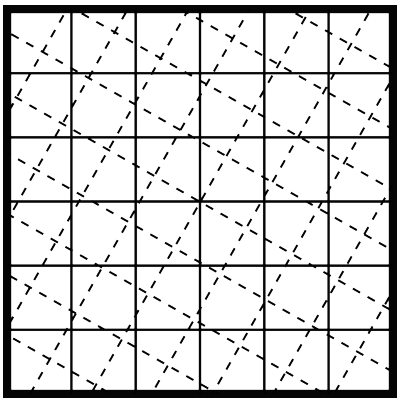

Figure 5: Schematic sketch of two lattices in one system. The system's boundaries are drawn with a thick solid line. While the boundaries are simple to describe in terms of coordinates of the solid thin lattice, the question whether a process on the dashed lattice crosses boundaries is more involved to answer algorithmically in terms of dashed coordinates.

of lattice kMC discussed under section 2.3.3, one needs a more general formulation.

In the following I will introduce an ml-kMC method in a recipe style. First I will explain the requirements that were considered for the implementation, second I will describe the solution chosen in this work.

COMMENSURABILITY Two lattices are said to be commensurate if the lattice vectors of one lattice can be transformed into the lattice vectors of the other lattice with a matrix that contains only integer numbers. [4, 73] For the method developed here we have to demand that all lattices modeled in a ml-kMC have one common commensurate superlattice. This in fact limits the set of problems we can tackle with ml-kMC.

INTEGER COORDINATES Once we have fixed one or more lattices to represent the adsorption sites, it is recommended to use integer coordinates since, *i.e.* each site is represented by tuple of integer numbers. The lattice is usually stored in an array and thus integers are the most natural way to address a site.

PERIODIC BOUNDARY CONDITIONS Since kMC is a computational method and any computer has a finite memory, one is limited to represent a finite system. Here it is common practice to use periodic boundary conditions. While periodic boundary conditions are straightforward to implement on a single rectangular lattice, it is more complicated for multiple lattices. Consider *e.g.* two orthogonal lattices that are rotated with respect to each other, as depicted in figure 5. If the boundaries of the system are parallel to the axis of one lattice, the same boundaries are usually non-trivial to describe in terms of the other lattice. Thus in a practical implementation the process list definition should not have to be aware of boundaries.

TRANSFERABILITY If successful on one system usually one will try to apply a solution on a different system. From this point of view the

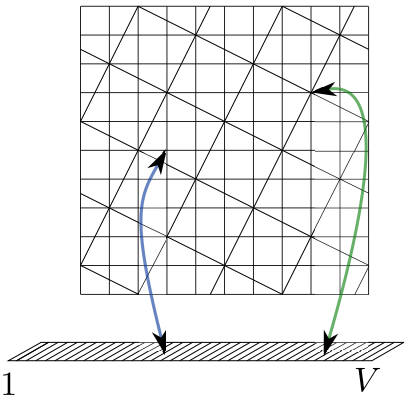

Figure 6: The mapping approach illustrated with two superimposed lattices. A generic kMC algorithm is implemented for a simple cubic hypercube in one dimension, while the process list is defined in terms of convenient lattice coordinates of the system. Periodic boundary conditions are implemented in the mapping.

recipe should be practical but also general enough, so that it can be directly applied to other combinations of lattices.

2.6.1 *General Recipe*

THE BASIC IDEA For each lattice enumerate all sites in the modeled system starting from 1. Or in more mathematical terms define for each lattice an injective mapping onto the simplest conceivable lattice: a simple-cubic hypercube in one dimension, see figure 6. The kMC algorithm (2.3) is then implemented on the 1-dimensional lattice while the actual process lists can be defined in terms of convenient coordinates.

RECIPE We are given two lattices $\mathbf{a} = \{\mathbf{a}_1 \dots \mathbf{a}_d\}$, $\mathbf{b} = \{\mathbf{b}_1 \dots \mathbf{b}_d\}$ in d dimensions motivated by the adsorption sites of two lattice structures.

Step 1 One has to ascertain that $\mathbf{a}$ and $\mathbf{b}$ are chosen such, that say each point on $\mathbf{a}$ can be assigned to a point in $\mathbf{b}$, or vice versa[6], while at the same time no points clash. That means any point in $\mathbf{a}$ cannot exist simultaneously with its corresponding point in $\mathbf{b}$ by the physics (or kinetics) of the system. If this is not satisfied, one needs to refine the mesh of one lattice until this can be satisfied.

Step 2 Fix a superlattice $\mathbf{A}$ (below simply referred to as superlattice having supercells) that is commensurate to $\mathbf{a}$ and $\mathbf{b}$ and a system size $\mathbf{T}$. [7] That means there are linear transformations $\mathbf{v}$, $\mathbf{w}$ with

$$\begin{aligned} \mathbf{A} &= \mathbf{v} \cdot \mathbf{a} \\ \mathbf{A} &= \mathbf{w} \cdot \mathbf{b} \end{aligned}$$

and $\det(\mathbf{v}), \det(\mathbf{w}) \in \mathbb{N}$.

6 This requirement is crucial if one wants to describe processes across lattice boundaries, *e.g.* diffusion of a particle from one lattice to the other. If this requirement is not fulfilled, one can use neither $\mathbf{a}$ nor $\mathbf{b}$ to describe the difference vector between affected sites.

7 The model system then has a size $\mathbf{T} \cdot \mathbf{A}$.

Step 3 Fix a mapping f_i with $i \in \{a, b\}$, *e.g.* implemented via a lookup table, that assigns a number to the local part, *i.e.* the part within a supercell in each lattice—and its reverse $\mathbf{f}_i^{-1}$. As mentioned under step 1 those should not clash and the set of numbers of one lattice should be a superset of the other set. We will refer to these mappings by

$$f_i : \mathbb{N}^d \to \mathbb{N}, \qquad \mathbf{f}_i^{-1} : \mathbb{N} \to \mathbb{N}^d.$$

Let n_l be the cardinality of the superset.

Step 4 Using all the definitions given above, we can state say the mapping from and to **a** in pseudo-code for $d = 2$.[8] Here % represents the modulo operation and / represents the integer division. For vectors they are to be applied componentwise.

Function a2nr

Input: site vector **n**
Output: index n
$\mathbf{N} = \mathbf{v}^{-1} \cdot \mathbf{n}$
$\mathbf{N}_0 = \mathbf{N}/1$ `// determine supercell`
$\mathbf{N}_r = \mathbf{N}_0 \% \mathbf{T}$ `// apply boundary condition`
return $\mathrm{f}_a\left(\mathbf{n} - \mathbf{N}_0 \cdot \mathbf{v}\right) + \left(\mathbf{N}_r\right)_1 \cdot n_l + \left(\mathbf{N}_r\right)_2 \cdot \left(\mathbf{T}\right)_1 \cdot n_l$

Function nr2a

Input: index n
Output: site vector **n**
$n_0 = n \% n_l$ `// determine number within supercell`
$S = n/n_l$ `// determine number of supercell`
$N_1 = S \% T_1$
$N_2 = S/T_1$ `// determine supercell`
return $\mathbf{f}_a^{-1}\left(n_0\right) + \mathbf{v} \cdot \mathbf{N}$

Generalization of the lattice KMC Algorithm

Based on this mapping an extension of the lattice kMC algorithm is straightforward. Processes on different lattices are listed as different entries in the process list and are implemented as different functions, *e.g.* `diffusion_co_right_pd100` and `diffusion_co_right_pdo`, which call the corresponding mapping function, when accessing the system's configuration. To ensure consistency of the program a useful trick is to represent identical species on different lattices with a different range of numbers, *e.g.* use $0, 1, 2, \ldots$ for species on one lattice and $10, 11, 12, \ldots$ for the corresponding species on another lattice.

After each process execution the local environment of a process is examined to check if lattice reconstructions need to be performed. If this is the case atoms are arranged and processes are enabled accord-

8 The extension to a higher dimension is straightforward. However limited memory poses a more severe restriction here.

ingly as stated below. For more details about the overall structure of the implementation, please see Appendix A.

Algorithm 2: ml-kMC

Fix rate constants k_{ij},
initial state x_i, and initial time t
while $t < t_{max}$ **do**
  Draw random numbers $R_1, R_2 \in]0, 1]$
  Find l such that $\sum_{j=1}^{l} k_{ij} < k_{i,tot} R_1 \leq \sum_{j=1}^{l+1} k_{ij}$
  Change state $x_i \rightarrow x_l$
  Increment time $t \rightarrow t - \frac{\ln(R_2)}{k_{i,tot}}$
  Reconstruct lattice if necessary
end

2.6.2 *Disclaimer*

Strictly speaking the current project is not the first to develop a multi-lattice kMC simulation. In other contexts researchers have been faced with the fact that one wants to describe a system with kMC that involves more than one lattice. Huang and Gilmer also describe a *mapping* approach to implement multi-lattice growth of thin films [74]. Bos performed a kMC simulation of a phase transition between bulk phases of iron [75, 76]. Whereas these studies use ml-kMC mainly to study the structure itself, in the present work chemical processes on an evolving structure are the main interest.

On the other hand other authors have recognized the challenge associated with geometric reconstruction and surface reactions in a lattice Monte Carlo simulation and found it prohibitive to model explicitly. Kortlüke *et al.* devoted a series of papers to model oscillatory behavior for CO oxidation on Pt(110) near the phase boundary of a surface reconstruction on a single lattice [77–81] but noted "[...] it is almost impossible to model a local change of geometry in lattice simulations [...] on a microscopic length scale [...]" [78, p. 2165]. Rogal notes "An explicit modeling of both phases including a reversible transition between them is therefore extremely involved." [27, p. 108].

2.6.3 *Other Applications*

The developed method is in principle applicable to various multi-lattice systems. Lundgren *et al.* reviewed surface oxides on Pd, Rh, Pt, and Ag. [24] They often feature comparable surface reconstructions, which could now be captured in a kMC simulation.

A different but closely related set of systems are model catalysts, where the interplay between active particle and substrate are essential to the functioning of the catalyst. An example of current interest are Nitrogen Storage Reduction (NSR) catalysts [82]. The interplay between a noble metal catalyst and a NOx storage material is essential, which provides for a typical multi-lattice problem.

Another example could be the open puzzle in the field of carbon nanotubes how one can predict and control the chirality of such tubes. [83] Tubes with different chirality have drastically different electronic properties. With ml-kMC one could possibly simulate growth on different substrates and test ideas of how to select chirality.

3 RESULTS

3.1 THE PDO/PD(100) MODEL

In this chapter we will use the developed multi-lattice kMC extension. The first half is devoted to motivate a model of CO oxidation on Palladium with an initial step of reconstruction. Next, I will show how this reconstruction may change surface coverage, oxide stability, and turn-over-frequency.

To simulate a transition from PdO to Pd(100) and back one has to come up with a reconstruction mechanism as well as process lists for these geometries. One intention of my project was to avoid extensive DFT calculations for setting up the model. The rationale is that even though ab initio calculations are inevitable for gaining predictive power, they would have easily exceeded the time frame of this work and tended to distract from the primary goal to demonstrate a working ml-kMC simulation. With this and the discussion under section 2.3.4 in mind the following construction should be regarded as a first attempt that evidently requires refinement assisted by ab initio methods.

I will now explain the key steps taken to motivate a first model. The main guide were geometrical DFT optimizations of a slab of a PdO layer on five layers of Pd(100) as depicted in figure 7. These calculations where provided by courtesy of J. Jelic deploying the Vienna Ab Initio Simulation Package (VASP) with a plane-wave basis set and the PW91 exchange-correlation functional. Further details can be found in her paper [84].

3.2 ADSORPTION SITES

The strategy to model new geometries is as follows: First one identifies high-symmetry sites, whose immediate environment is known from literature or at least very similar to those and find adsorbing species and binding energies. From this one can calculate adsorption and desorption rate constants. Then one identifies nearest neighbor sites and assigns two-site processes like diffusion, reaction, dissociative adsorption, or associative desorption.

Accordingly one should first establish, which adsorption sites are known. Palladium crystallizes in a face-centered cubic (fcc) structure. This means that the (100) surface is a simple cubic lattice in $d = 2$ dimensions. For clean Palladium under ultra high vacuum conditions surface relaxation is reported but no reconstruction. [85] Therefore one expects Palladium atoms to bind on hollow sites of Pd(100). Oxygen has been described to adsorb on hollow sites as well as long as no reconstructions at higher coverage take place. [19, 20] CO binds on the bridge site (carbon down). [86, 87] These findings were also reproduced with ab initio methods by Rogal *et al.*. [27]

For the PdO($\sqrt{5} \times \sqrt{5}$)$R27^\circ$ surface oxide layer experimental results in the literature about adsorption sites are sparse. This study therefore relies on Rogal's *et al.* ab initio study. Here oxygen binds most favor-

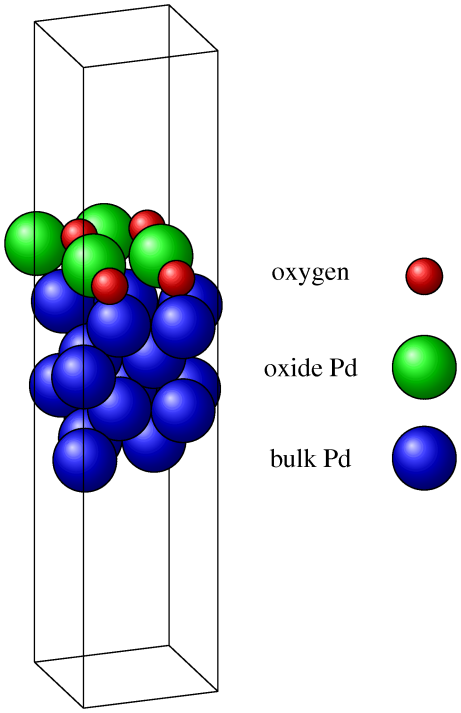

Figure 7: Slab geometry of PdO on Pd(100) used to calculate stable surface structures.

ably on the hollow site (usually considered part of the surface oxide structure) but also adsorbs on the PdO bridge site. CO binds most favorably to the PdO bridge sites, while it can also replace oxygen atoms on the PdO hollow sites.

3.3 GEOMETRIC CONSIDERATIONS

One can deduce two conjectures from this geometry of a PdO layer on top of bulk Palladium: One can hypothesize where Pd atoms shift during reconstruction and how large the cell needs to be to model the reconstruction mechanism. Figure 8 shows such a geometry together with high-symmetry points of the underlying bulk structure.

As one can see Palladium atoms labeled 1 and 3 in the oxide layer sit on or very close to Pd(100) hollow sites, that they would also occupy if there was no oxygen. In case the oxide layer becomes depleted of oxygen we therefore suspect that Palladium atoms move to this nearest hollow site. However, Palladium atoms 2 and 4 sit close to a bridge site and can potentially move to two different hollow sites, respectively, in the Pd(100) phase.

The two Palladium atoms on bridge together with the Palladium atoms on hollow make up one supercell which in turn makes up the entire lattice by mere repetition in two directions. Once we understand how these four atoms rearrange under oxygen depletion we are likely to understand the transition behavior of the entire lattice. So despite the number of possible reactions paths one might envision a required supercell that is remarkably small.

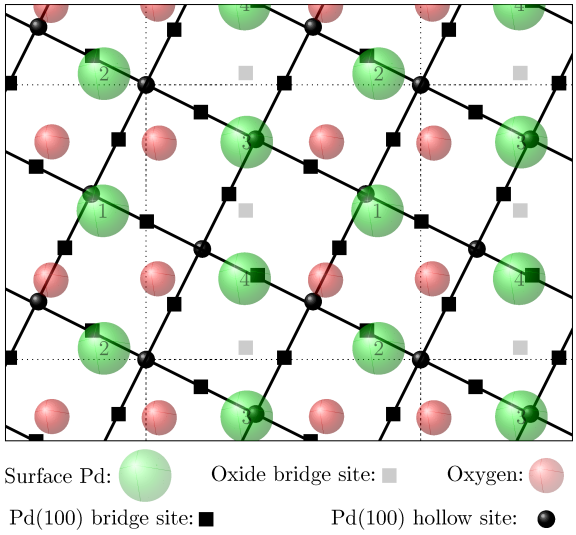

(a) top view

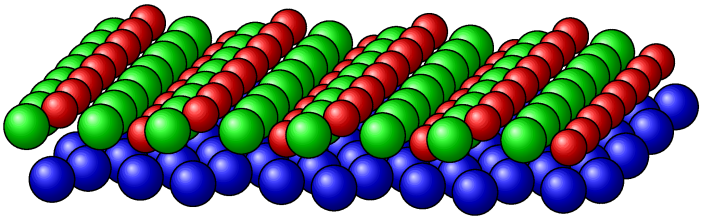

(b) side view

Figure 8: Pd oxide and Pd(100) stacked on top of each other in the upper panel. The black spheres and squares represent adsorption sites. This means substrate atoms are in the center of the thich black grid.

3.4 STRUCTURAL OPTIMIZATIONS

In order to obtain a first idea how the surface oxide responds to oxygen vacancies we started from the PdO structure, removed one oxygen atom, and performed a structural optimization using DFT. Removing only one of the four atoms per supercell never changed the geometry significantly, see figures 9-12. Here it is important to keep in mind that structural optimizations can only find the nearest local minimum on a downhill path on the potential energy surface.

Removing two atoms caused reconstructions. This reconstruction can be expected from a crude mean field approximation. The oxygen adsorption structure with the highest reported oxygen density on Pd(100) is $c\,(2\times 2)$[19, 20], which corresponds to $\frac{1}{2}$ monolayer of oxygen. The $(\sqrt{5}\times\sqrt{5})R27^\circ$ oxide reconstruction corresponds to an oxygen coverage of $\frac{4}{5}$ monolayer. Removing two oxygen atoms from each oxide unit cell corresponds to changing the local oxygen coverage from $\frac{3}{5}$ monolayer to $\frac{2}{5}$ monolayer, which is less than $\frac{1}{2}$ monolayer.

Before proceeding with removing all six combinations of two oxygen atoms in a unit cell and performing structural optimizations, we can rule out improbable paths. Even though upper and lower oxygen atoms have very similar binding energies [27], any process that removes lower oxygen atoms would have to displace Palladium atoms (see figure 8), which suggests considerably higher reaction barriers. Therefore a divacancy of two top oxygen atoms seems as an initial

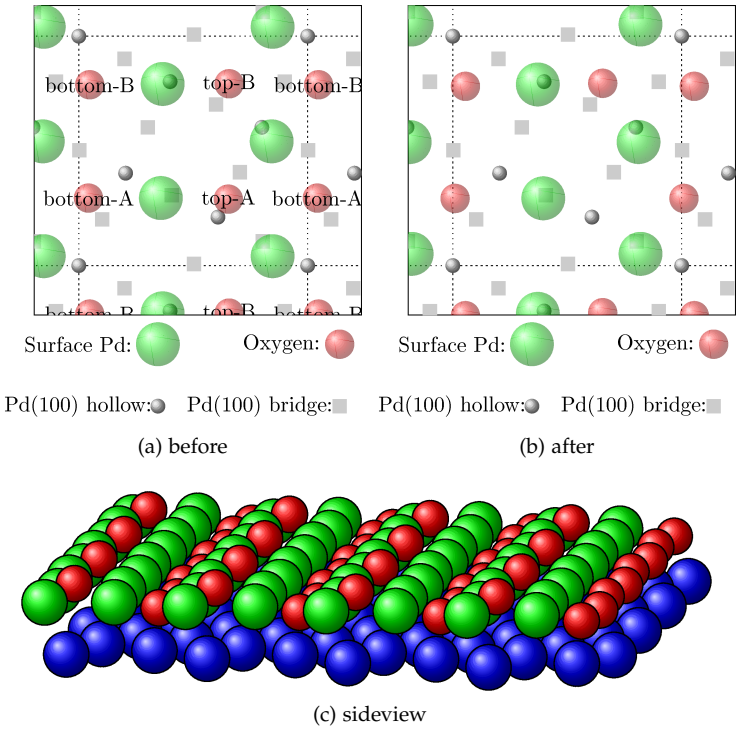

(a) before (b) after

(c) sideview

Figure 9: Optimized structure with a vacancy at the top-A oxygen position.

step of oxide destruction most likely. Figure 13 shows a structural optimization with both top oxygen atoms removed in one supercell surrounded by Palladium oxide.

As one can see all four Palladium atoms have shifted very close to hollow sites of the underlying Pd(100) structure, while the lower oxygen atoms are still below the top layer of Palladium. It is not possible to determine from a (1×1) unit cell, in which direction the unstable Palladium atoms slide. So we arbitrarily choose the direction towards the standard supercell. If this turns out critical, this could eventually be determined from a (2×2) calculation. From this, we derive the first central rule of reconstruction for the scope of this study (also refer to figure 14).

3.5 MODEL FOR RECONSTRUCTION

If an oxygen divacancy of two neighboring top oxygen atoms occurs, the neighboring Pd atoms reconstruct instantly forming a Pd(100) nucleus.

A schematic representation of the reconstruction rule including all newly created adsorption sites is depicted in figure 14. The situation is further complicated due to the possible presence of CO molecules. There are in total 36 combinations of empty and CO on the four affected sites. Since more CO corresponds to more oxide reducing conditions I do not expect CO to inhibit reconstruction. Instead we allow reconstruction and assign CO from destroyed sites to the nearest newly created bridge site on the Pd(100) nucleus. In practice this means that CO molecules merely follow the movement of their neighboring Pd atoms below.

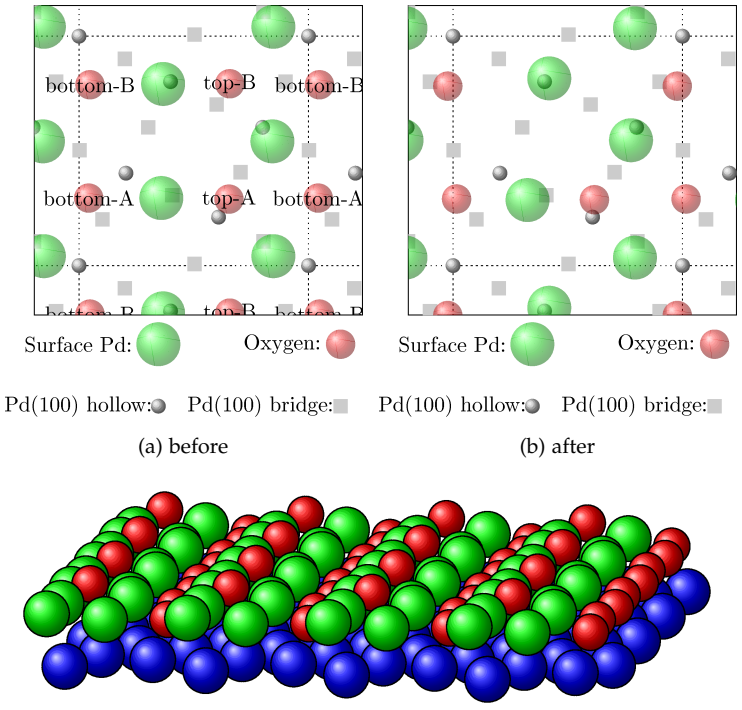

(a) before

(b) after

(c) sideview

Figure 10: Optimized structure with a vacancy at the top-B oxygen position

On the other hand the diffusion barrier for oxygen on the surface oxide to a neighboring hollow site is only 0.1 eV, which corresponds in the considered regime of 300 K-600 K to rates of the order of 10^{11} s^{-1}-10^{12} s^{-1}, respectively. We therefore assume that in case of a divacancy with oxygen on a neighboring bridge site, the oxygen atom will diffuse to the hollow site instantly and thereby inhibit oxide destruction.

A detailed listing of all reconstruction rules that result immediately from these considerations can be found in table 1 and the labels refer to those in figure 14.

3.6 DECONSTRUCTION REVERSAL

The ultimate goal of the PdO/Pd(100) model is to implement a complete but reversible transition from PdO to Pd(100). Thus it is foresighted to include reversing mechanisms in each step. Moreover if reversing mechanisms are not included one very quickly ends in an unphysical regime. If the temperature is just great enough that reconstructions occur, eventually the oxide will be completely destructed if the simulation runs long enough—and stay destructed for all times. That means one effectively imposes an infitely large hysteresis.

So far the model includes only one reconstruction rule. The two lower oxygen atoms are considered inactive. Adding a single oxygen atom again changes the local oxygen cover from $\frac{2}{5}$ of a monolayer to $\frac{3}{5}$ of a monolayer. From this we deduce the reverse mechanism for the first destruction step, which can only occur if the three neighboring bridge sites have not been occupied by CO (also refer to figure 15):

Table 1: Exhaustive list of possible configuration, that could lead to initial reconstruction replacement rules. For cases, where molecules are moved a rule is given by (species)@(old_sites)→(new_site). The labels are explained in figure 14. If the replacement leads to interruption of the reconstruction, this is expressed by `break`. Cases that are not expected to occur are marked with ↯.

A	*B*	*C*	*D*	Rule	#
-	-	-	-		1
-	-	-	CO	CO@D→d	2
-	-	-	O	O@D→B; `break`	3
-	-	CO	-	CO@C→c	4
-	-	CO	CO	CO@C→c; CO@D→d	5
-	-	CO	O	O@D→B; `break`	6
-	-	O	-	O@C→A; `break`	7
-	-	O	CO	O@C→A; `break`	8
-	-	O	O	O@C→A; O@D→B; `break`	9
-	CO	-	-	CO@B→e	10
-	CO	-	CO	CO@B→e; CO@D→c	11
-	CO	-	O	CO@B→A; O@D→B; `break`	12
-	CO	CO	-	CO@B→e; CO@C→c	13
-	CO	CO	CO	CO@B→e; CO@C→c; CO@D→d	14
-	CO	CO	O	CO@B→A; O@D→B; `break`	15
-	CO	O	-	O@C→A; `break`	16
-	CO	O	CO	O@C→A; `break`	17
-	CO	O	O	O@C→A; O@D→B; `break`	18
CO	-	-	-	CO@A→b	19
CO	-	-	CO	CO@A→b; CO@D→d	20
CO	-	-	O	O@D→B; `break`	21
CO	-	CO	-	CO@A→b; CO@C→c	22
CO	-	CO	CO	CO@A→b; CO@C→c; CO@D→d	23
CO	-	CO	O	O@D→B; `break`	24
CO	-	O	-	O@C→B; `break`	25
CO	-	O	CO	O@C→B; `break`	26
CO	-	O	O	O@C→B; `break`	27
CO	CO	-	-	↯	28
CO	CO	-	CO	↯	29
CO	CO	-	O	↯	30
CO	CO	CO	-	↯	31
CO	CO	CO	CO	↯	32
CO	CO	CO	O	↯	33
CO	CO	O	-	↯	34
CO	CO	O	CO	↯	35
CO	CO	O	O	↯	36

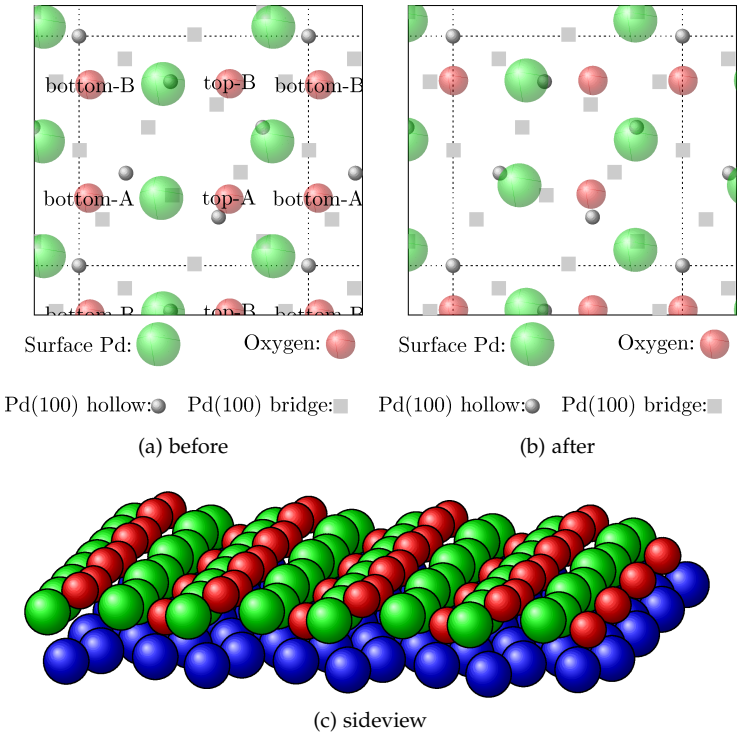

(a) before

(b) after

(c) sideview

Figure 11: Optimized structure with a vacancy at the bottom-A oxygen position

The local destruction of the oxide is reversed if oxygen binds on the new Pd(100) hollow site.

The processes that can lead to or hinder this configuration are explained in the following section.

Process Between PdO and Pd(100) Nucleus

Oxygen processes: There are in total 4 processes considered of how oxygen can come to rest in the Pd(100) nucleus hollow site: two adsorption processes and two diffusion processes:

- Diffusion from the neighboring oxide bridge and hollow site: the barriers are estimated from interpolating the respective PdO and Pd(100) barriers.
- Dissociative O_2 adsorption on the same sites: the rate constants are assumed to be identical with the corresponding rates on PdO.

Oxygen processes with sites on the lower edge of the hole seem unlikely due to the comparably large distance and will not be considered.

As mentionend above: in all cases oxygen can only come to rest on the Pd(100) hollow site, if the three neighboring bridge sites are not occupied with CO since they would be prohibitively close. This may hinder the reversal of oxide destruction.

CO processes: the processes of CO within the Pd(100) nucleus are assumed to be identical with the extended Pd(100) subsystem.

There are additional CO processes between PdO and Pd(100), which can be divided into diffusion over the top edge and diffusion over the bottom edge. Both are indicated in figure 16:

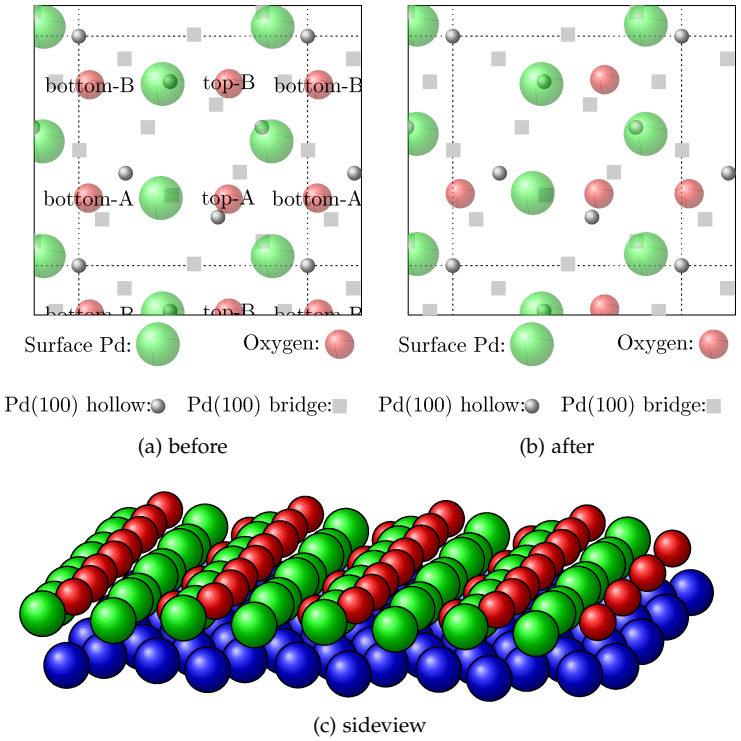

(a) before (b) after

(c) sideview

Figure 12: Optimized structure with a vacancy at the bottom-B oxygen position

- Diffusion from oxide to metal: the barriers are estimated from interpolating the respective PdO and Pd(100) barriers.
- Diffusion from metal to oxide: the barriers are estimated from interpolating the respective PdO and Pd(100) barriers.

The indicated correction for diffusion rates might bear an important effect: the fact that the oxide binds CO more strongly has an effect of removing CO quicker from the Pd(100) nucleus, which yields space for oxygen to adsorb on the nucleus and reverse the destruction. The opposite case (meaning CO binds stronger on Pd(100) than on PdO) would mean that a single hole in the oxide could have catastrophic effects for the oxide. This could explain how the oxide layer recovers from destruction. For a coarse-grained overview of the modeled reconstruction please refer to figure 17.

Possible reactions between CO on the Pd(100) nucleus and oxygen on oxide sites are not considered.

Modeling of Diffusion Barriers

Diffusion barriers between Pd(100) sites and PdO for CO and oxygen have not been calculated so far to the best of my knowlede. To shortcut lengthy calculations as a first crude approach we assume that the interlattice saddle point is energetically halfway between the two known saddle points. The energy landscape is depicted schematically in figure 18 and the resulting barrier is highlighted in gray. In the case of oxygen diffusion from PdO bridge to Pd(100) hollow the arithmetic mean is energetically lower than the PdO site, so I choose the PdO

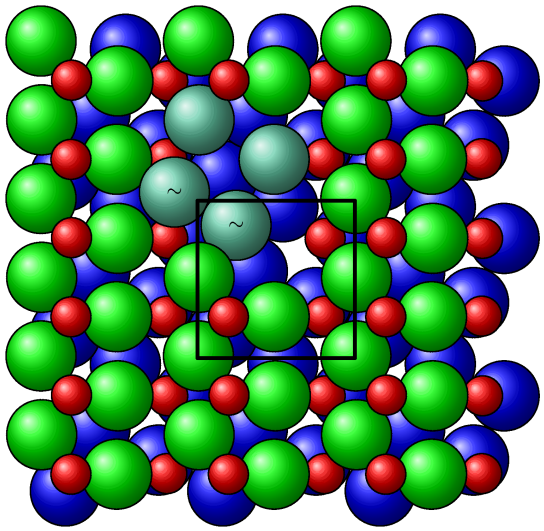

Figure 13: Reconstructed supercell surrounded by unreconstructed supercells

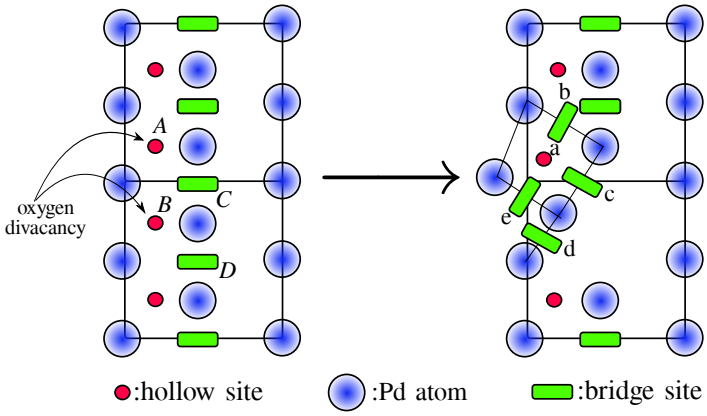

Figure 14: Reconstruction rule and reconstructed geometry

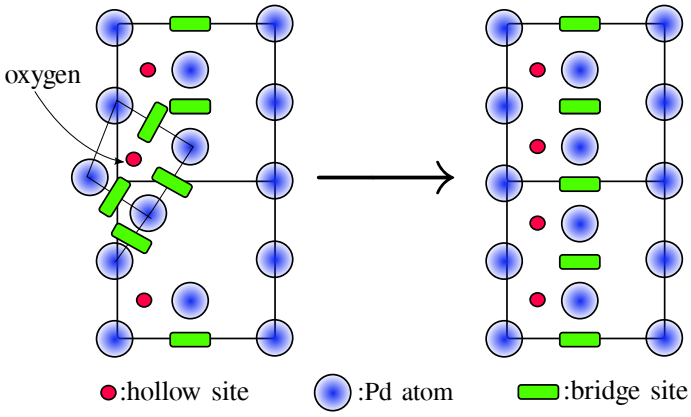

Figure 15: Rule for reverse of reconstruction

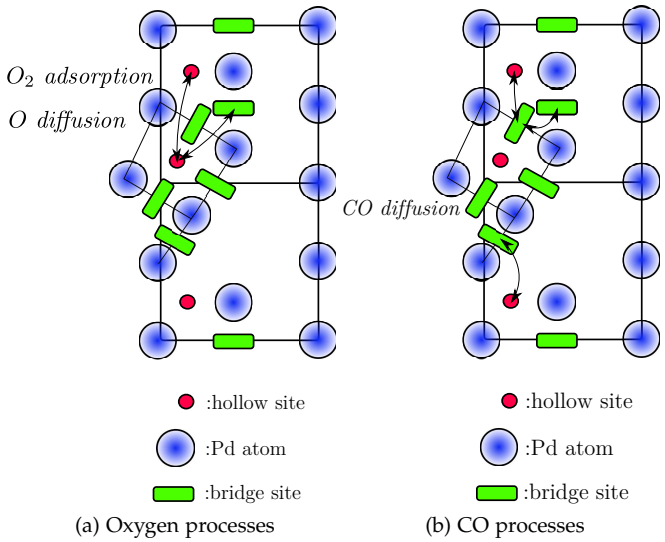

(a) Oxygen processes (b) CO processes

Figure 16: New processes between oxide and the Pd(100) nucleus

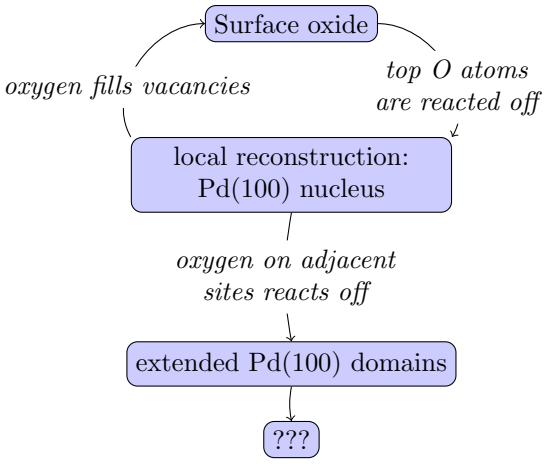

Figure 17: Schematic reaction pathway

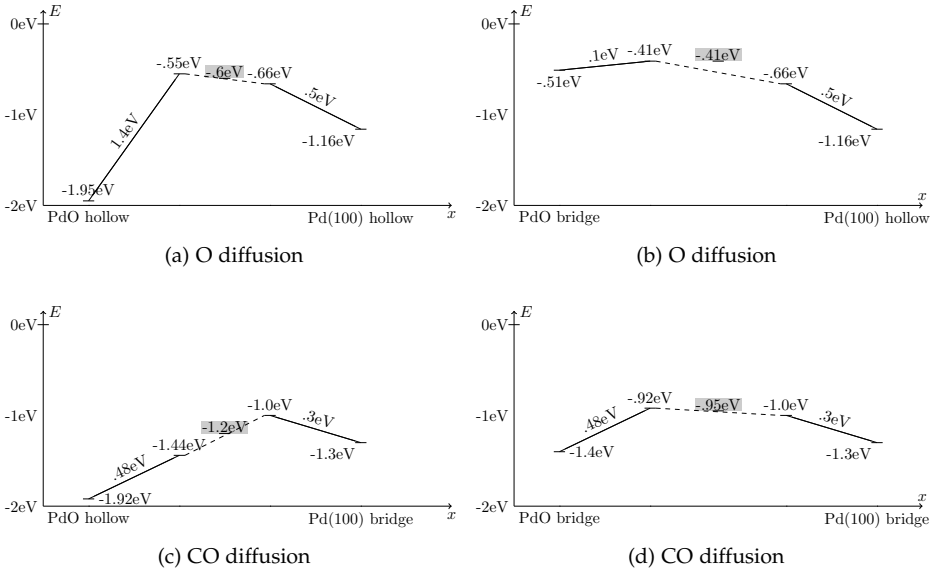

Figure 18: Schematic illustration of the saddle point interpolation used to determine interphase barriers. The binding energies with respect to the vacuum level of the adsorption sites are given to the very left and right. Moving to the center the diffusion barrier on the respective lattice is added resulting in the energy of the respective transition state. We then assume that the transition state at the phase boundary is energetically halfway between the two transition states.

diffusion barrier as the saddle point to circumvent negative barriers. If desired an electronic structure calculation could answer if the PdO at an edge is a stable adsorption site for oxygen at all. In practice oxygen on PdO bridge will diffuse to Pd(100) hollow almost immediately in either case and thereby reverse the oxide destruction.

3.7 ML-KMC AND DETAILED BALANCE

When one tries to apply the principle of detailed balance to the reconstruction below one encounters difficulties, which seem symptomatic for this variant of ml-kMC. The anticipated reconstructing process always occurs instantly, when a certain local configuration is encountered. There is no reverse process and therefore detailed-balance seems not applicable!

This conundrum can be understood, when we change the point of view. Consider we where metallurgists and only interested in the structure of Palladium while oxygen and CO where only some perturbation that induces a change to the structure. Then the process list would probably consist of various self-diffusion hops. The aforementioned oxide to metal reconstruction would be a hop without a barrier, *i.e.* not-activated, and the final state would be energetically well below the initial state. Therefore the forward process occurs nearly instantly whereas the reverse occurs rarely or not at all because it is energetically very unfavorable.

This picture supports our modeled reconstruction well. However it leaves us with an open question of how the released potential energy decays after a reconstruction. We assume for now that it quickly dissipates into the bulk or other decay channels. If the released energy

is large enough, one could imagine that adatoms are *e.g.* excited to higher vibrational states and transition rates are locally enhanced for a certain time until energy has dissipated into the bulk.

3.8 SUMMARY OF THE MODEL

This section contained various considerations on different levels of detail. It seems justified to summarize the essential features.

For practitioners all details of the model are contained in Appendix B and table 1. Assuming a general understanding of kMC one should be able to repeat this computer experiment with this information.

On a more abstract level the model is characterized as follows: It is based in Rogal's PdO lattice model (as described in the dissertation [27] or refer to Appendix B), but without lateral interaction plus a reversible local reconstruction rule.

Rogal's model consists of alternating columns of bridge and hollow sites, which are characterized by different binding energies and barriers. Two site processes only occur between pairs of a hollow column and one adjacing bridge column. In this way the lattice is an array of quasi 1-dimensional subsystems (see Appendix B). On these subsystems we allow the usual four process types adsorption, desorption, diffusion, and reaction to occur between nearest neighbors; given of course that the local configuration allows for it.

The reconstruction rule applies if two adjacent hollow sites are not occupied by oxygen and rearranges two Palladium atoms in such a way that four Palladium atoms form a minimal Pd(100) like structure. This rearrangement is reversed if an additional oxygen atom is present.

The Pd(100) part of the model is, yet, very elementary. It includes CO adsorption, CO diffusion within the nucleus and between Pd(100) and neighboring PdO sites as well as dissociative O_2 adsorption with neighboring PdO sites and oxygen diffusion from PdO. CO and oxygen cannot simultaneously adsorb on the Pd(100) nucleus since they either block each other or the presence of oxygen reverts the nucleus to the PdO structure. Reactions between species on PdO and Pd(100) are at present omitted.

3.9 SIMULATION RESULTS

3.9.1 *Occupation Benchmark*

The developed model without the possibility of reconstruction is a simplified version of Rogal's model. As an initial check I compared the coverage resulting from both implementations under identical conditions. Therefore I set the lateral interaction energies in the existing code to zero and disabled any reconstruction rules in my implementation. Then I compared the occupation for a range of temperatures.

Here and in the following simulations are performed on a lattice of 20×20 supercells. In the formulation of Rogal's PdO model this corresponds to 20×40 sites, since each PdO/Pd(100) supercell contains two PdO supercells. Selective tests on larger lattices showed that the small lattice size introduced fluctuations in evaluated observables but did not shift values systematically. Several tests where performed to make sure that, that steady-state was reached before observables are evaluated. Testing for various conditions it was found that after 32

million kMC steps steady state was certainly reached. Therefore for each calculation 32 million steps where carried out first, then averages where taken over 1-2 million kMC steps.

The results can be seen in figure 19 and figure 20. Since the curves agree almost perfectly all further simulations are performed with the newly developed program.

The general trend that at higher temperatures the oxide is stable for a higher CO partial pressure is reproduced. However neglecting lateral interations shifts the transition of oxygen depletion to considerably lower CO partial pressures compared to the original model of Rogal[27]. This shows that lateral interactions cannot be neglected on PdO when aiming for a quantitave modeling of the phase boundary.

3.9.2 *Oxide Stability*

Rogal used oxygen occupation of upper PdO hollow sites as an indicator for the stability of the surface oxide. A relative occupation of 0.9 was chosen *ad hoc* as a warrant of surface oxide stability. In the new model local oxygen depletion of these sites is chosen as a precursor of oxide destruction. In this view it is trivial that the new model supports the previous descriptor in general. However, with an explicit but local reconstruction mechanism, we can estimate better how well the 0.9 relative occupation was chosen. In figure 21 the surface coverages are shown together with the average relative number of unreconstructed supercells.

For the examined temperatures the choice of 0.9 relative occupation seems quite safe. Here the relative oxidation barely deviates from 1., which corresponds to a complete surface oxide layer. Considering a certain fraction of unreconstructed supercells as a new warrant for oxide stability only pushes the *ad hoc* criterium one notch further since the model still cannot represent the full destruction of a surface oxide. However we say that introducing an explicit reconstruction step does not lower the CO partial at which the oxygen occupation of the upper hollow sites drops at $T = 600$ K. Based on Rogals results [27, pp. 125], *i.e.* taking into account the overall shift of pressure due to the omission of lateral interactions, one can deduce that at a stoichiometric feed of oxygen and CO reactants a surface oxide layer on Palladium is stable.

3.9.3 *Turn-over-frequency*

The last observable we turn to is the turn-over-frequency (TOF) of $CO + \frac{1}{2}O_2 \rightarrow CO_2$. A comparison between the PdO/Pd(100) model with and without reconstruction (*i.e.* the PdO) model is given in figure 22. Since the reconstruction rule seems to increase the turn-over-frequency at optimal CO partial pressure by a remarkable factor of three at 600 K, one should try understand the mechanism behind this.

In order to do this we fix 600 K as a temperature and plot the TOF together with the occupation of different sites as a function of CO partial pressure, see figure 22. As one increases the CO partial pressure, surface occupations start to deviate from their low-CO limits at identical values of roughly $p_{CO} \approx 2 \cdot 10^{-3}$ bar. However in the case of no reconstruction oxygen occupation drops abruptly after this yielding to CO, while in case of allowed reconstructions the oxygen depletion is delayed considerably. In the latter case CO occupation on PdO sites

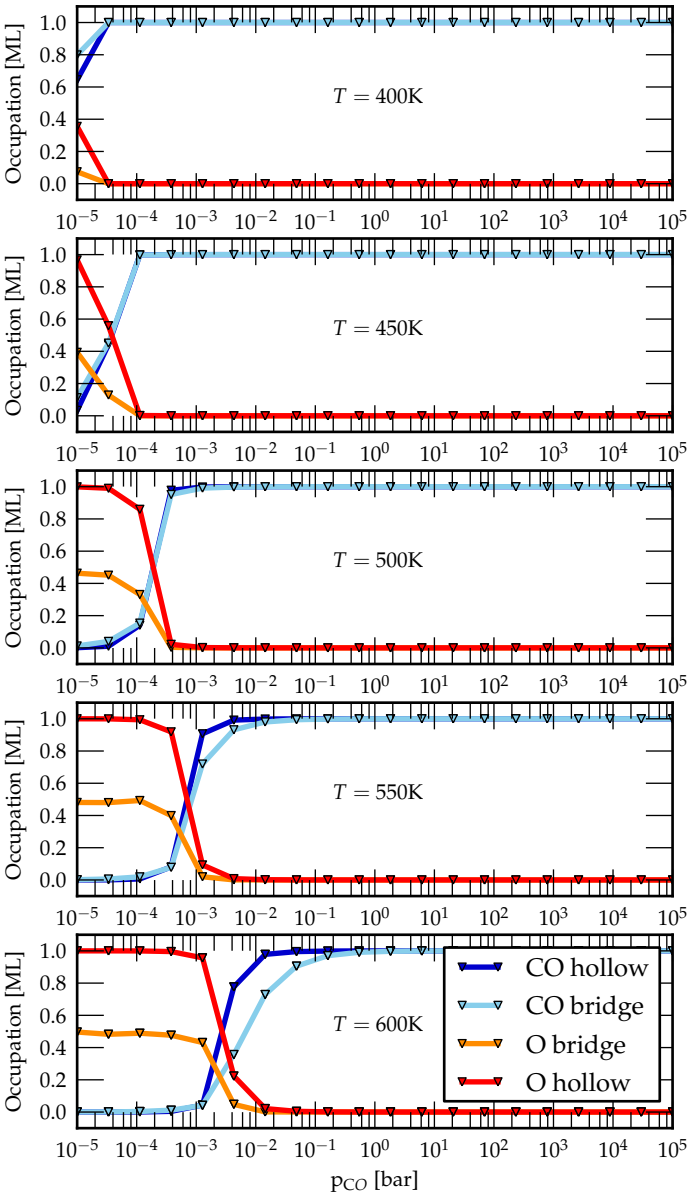

Figure 19: Occupation of various sites and species from Rogal's implementation [27].

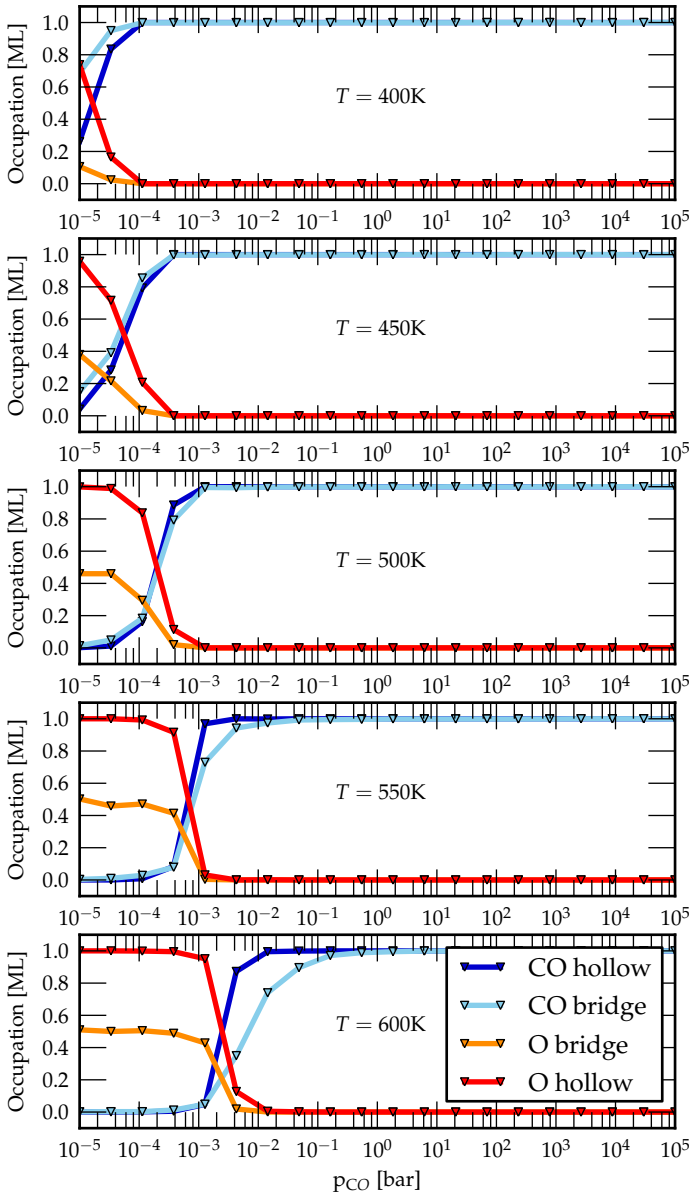

Figure 20: Occupation of various sites and species from the present implementation.

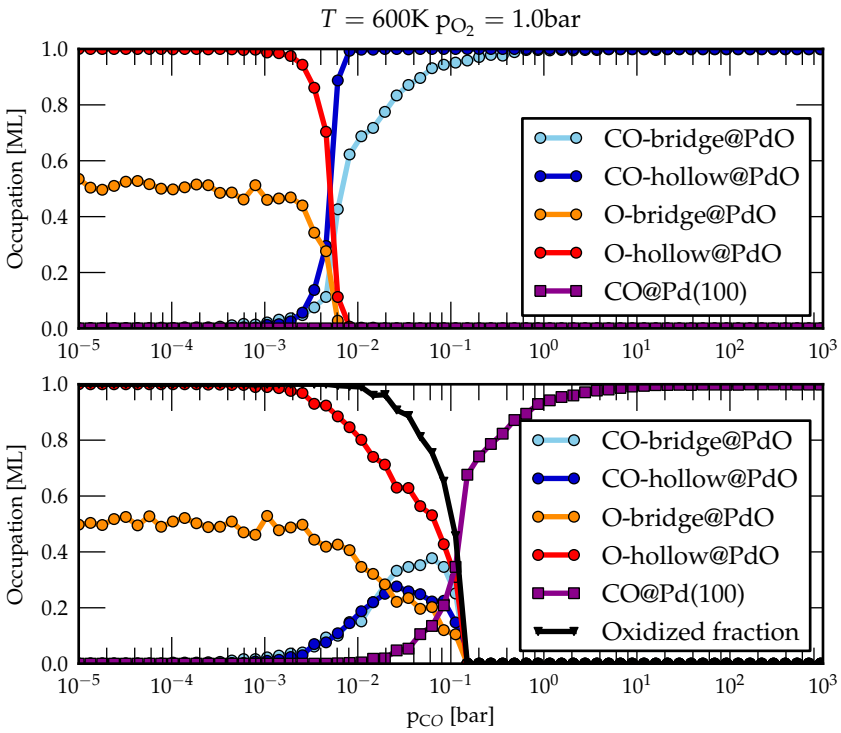

(a)

Figure 21: Analysis of oxygen coverage of upper hollow sites as a descriptor for oxidation. The top panel shows the occupation of different surface site in monolayers without allowed reconstruction. The bottom shows the occupations as well as the average fraction of supercells that are not reconstructed to a Pd(100) nucleus, *i.e.* have an oxidic configuration. This plot demonstrates that including an atomistic reconstruction mechanism shifts the CO partial pressure needed for an onset of oxide destruction to higher pressures.

builds up until it reaches $p_{CO} \approx 0.07$ bar and drops abruptly, which is when the oxidic structure collapses altogether and CO occupation of Pd(100) sites dominates. There is no oxygen occupation of Pd(100) sites, since this is not allowed by the model.

One should stress the speculative nature of this result. It is most likely a by-product of a half-finished model. Furthermore the effect most likely occurs only due to the omission of lateral interactions. If the transition actually occurs at CO partial pressures above stoichiometric feed, as concluded in the previous section, this reconstruction effect does not occur at all.

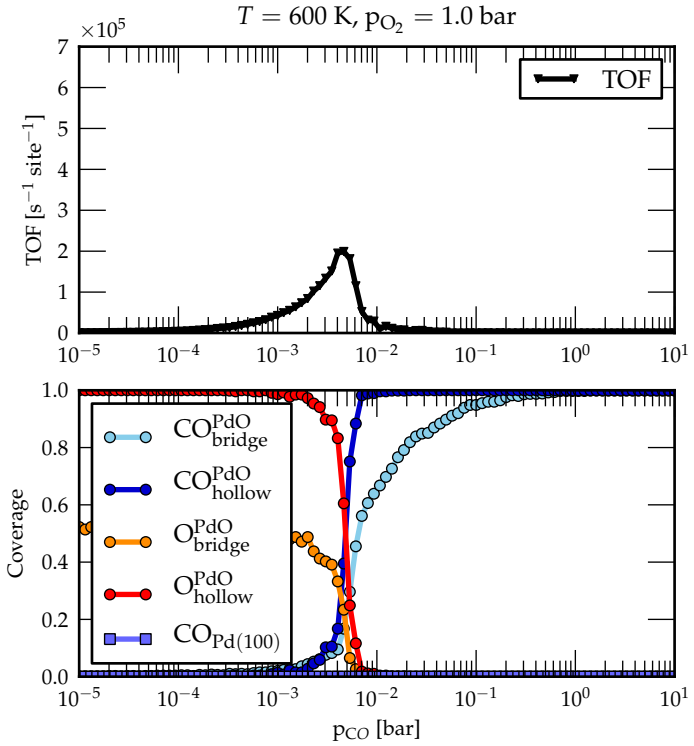

(a) without reconstruction

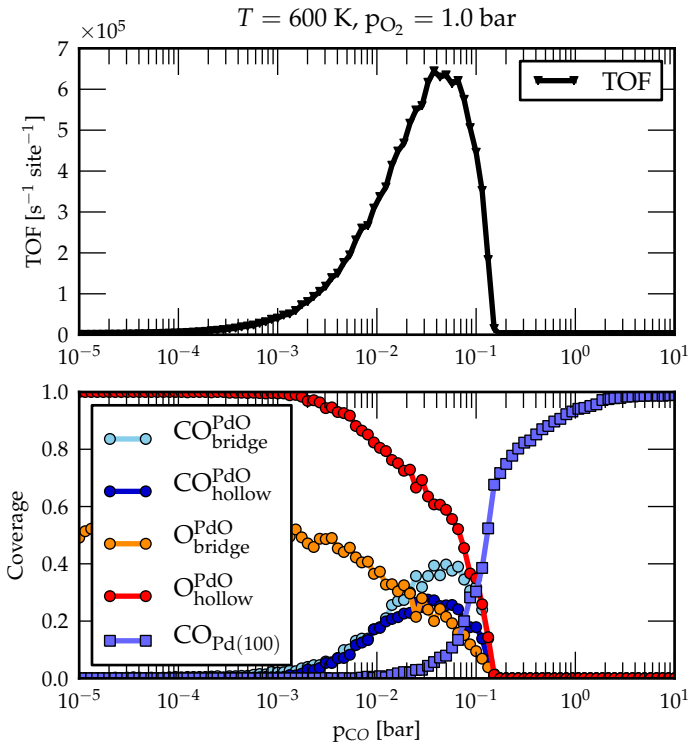

(b) with reconstruction

Figure 22: Turn-over-frequencies together with surface occupation. In the case without reconstruction the CO on Pd(100) occupation trivially remains 0 ML, while in the extended model CO eventually replaces all other surface species. This implies the complete destruction of the oxide. In this model the reconstruction rule actually shifts the oxide destruction to higher CO partial pressures. In the present model with no lateral interaction this improves the reactivity since the most stoichiometric conditions on the surface occur closer to a stoichiometric gas feed.

4 SUMMARY AND OUTLOOK

4.1 SUMMARY

In summary I think it is fair to say, that we took an important step to unravel the reactivity of Palladium. The formulation of multi-lattice kinetic Monte Carlo given above can model the kinetics at the phase transition quite directly and is now ready to be supplemented with detailed first-principles energetics. The computational cost of the ml-kMC simulations themselves is comparable to single-lattice simulations. Thus the algorithmic efficiency of lattice kMC can now be used on a new class of problems, *viz.* we are now in a position to specifically address the reaction kinetics during an ongoing reconstructive phase transition such as oxidation of a solid-state catalyst.

With the help of DFT based structural optimizations we obtained a new atomistic model of the onset of a Palladium surface oxide destruction and its reversal.

The results for the oxidic fraction support Rogal's predicted boundaries taking into account the additional approximations. The lack of lateral interactions causes the Palladium oxide to be more vulnerable to destruction but the trend that higher temperatures improve oxide stability is observed as well. Furthermore it could be validated that the assumption that the surface oxide is stable for an occupation of the upper hollow sites of 0.9 relative occupation or more that was introduced *ad hoc* in Rogal's preceding work holds even when introducing an atomistic oxide destruction step. This underlines that at stoichiometric feed for CO oxidation and elevated temperature ($\sim$ 600 K) a thin surface oxide should be the active phase.

4.2 OUTLOOK

There are two directions to improve the PdO/Pd(100) model as it is. On the one hand one should verify from electronic structure calculation the assumptions made in the reconstruction mechanism. On the other hand the reconstruction process should be expanded ideally up to extended Pd(100) domains at the surface. To fully demystify the active site of Palladium for CO oxidation at technological gas-phase conditions one needs to follow both.

To verify the existing model one could deploy *ab initio* molecular dynamics at finite temperature to find out how Palladium atoms actually respond to removing one or two oxygen atoms under thermal excitation. Ideally this simulation would be done in larger unit cells, where the oxygen vacancy is surrounded by one intact supercell in each direction. As this might quickly become quite expensive a first step could already be to verify the correction with structure optimizations on a larger unit cell. Since simulations have shown that the effect of oxide reconstruction is very sensitive to the binding energies of the newly created sites, precise calculations of these should be a high priority.

If these *ab initio* methods verify the reconstruction modeled so far the logical next step is to extend the model to include further recon-

struction steps. CO oxidation reactions between species on Palladium oxide and Pd(100) like patches have not been considered yet. *Ab initio* transition state searches such as nudged elastic band (NEB) [88] will be necessary to calculate reaction barriers.

One problem here is that due to the increasing complexity of the metal to oxide interface more than one set of initial positions will have to be considered.

The next problem would be to tackle the lower oxygen atoms in the thin surface oxide layer. As the Palladium oxide layer structure becomes more and more rearranged one can expect that these lower oxygen atoms become accessible to diffusion, reaction, or desorption, too. As this fully destroys the oxide layer the most important aspect might be to predict the reverse process of this oxygen removal. This answer would imply the initial phase of oxide formation. The often discussed subsurface oxygen alludes that oxygen diffuses into the bulk, as *e.g.* observed for hydrogen [89]. Since this seems not so likely for oxygen on a perfect Pd(100) surface [90, 91], an alternative is, yet, to be found. Here a series of kMC simulations with the fraction of movable Palladium atoms in the surface layer as a parameter could give important answers.

This situation is further complicated by the fact that Palladium apparently shows quite fast self-diffusion. Kim *et al.* calculated self-diffusion barriers, that include hopping and exchange mechanisms, by means of molecular dynamics, and found barriers as low as 0.62 eV and 0.35 eV on flat surfaces and steps, respectively. [92, 93] Thus, the diffusion occurs on the same time-scale as the one of oxygen or even CO. Starting from the metallic lattice the oxide can grow at several translationally invariant positions of the Pd(100) lattice, which would lead to domains of horizontally shifted oxide patches.

Another aspect that would need to be investigated is the latent heat that is set free at this reconstructive phase transition and possible decay channels of it. If this latent heat does not directly dissipate into the bulk but say cause vibrational excitation of neighboring adatoms one could map this effect onto kMC with an effective rate since a barrier might look effectively lower for a vibrating atom.

These qualitative considerations show already some of the complexities of modeling a surface phase transition in practice. A comprehensive modeling still takes considerable amount of work. The present study shows that such questions can be dealt with using multi-lattice kMC as one part of the tool chain. The realization of this will take further effort, but the feasibility has been proven.

A

EFFICIENT, MODULAR KMC

This appendix summarizes key aspects of the developed kMC program. I had two questions in mind when developing this framework regarding efficiency : *How efficient is it to implement a new kMC model or modify an existing one?* and *How efficient is the resulting implementation?*

KMC is often praised for its efficiency. That is because the covered time scales are far greater than in typical molecular dynamics. Yet, if the method is powerful and calculations are cheap, why does it still take months to develop and perform a kMC simulation? Or in Wilson's words "Where is the real bottleneck in scientific computing?". [94]

KMC simulations are intrinsically difficult to debug. Typical programming errors do not lead to dramatic events such as a division by zero, diverging observables or singular matrices known from other computational methods. The typical programming error leads to slightly modified kinetics and can easily go unnoticed or worse be interpreted as interesting physics. Searching for these kind of errors is anything but efficient.

KMC Modularization

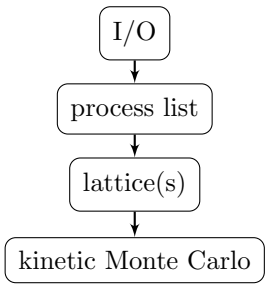

Figure 23: The modularization chosen for the kMC program

The program is structured into 4 modules as depicted in figure (23). The idea behind this is to separate code into different levels of generality and reusability.

GENERIC KINETIC MONTE CARLO At the lowest level is the kMC solver. This module performs the elementary tasks of selecting the next process and propagating time. It contains no geometrical information of a specific model and be used for arbitrary (multi-) lattice kMC simulations in as many dimensions as desired. Utility functions such as a reload mechanism and memory (de)allocation are also provided.

LATTICE(S) The second module provides all geometrical information. It relies on a suitable mapping such as the one described in

section 2.6.1 and replicates all methods of the underlying module in terms of crystal lattice coordinates.

PROCESS LIST The third module describes all processes that can take place on this lattice. This part changes fairly frequently, for instance each time one includes additional processes.

The intuitive way to describe a process is to define *conditions* and *actions*. Accordingly one might say something like "If site A is occupied by X and its nearest-neighbor site B is empty, then X can diffuse from A to B with a given rate". However such a description is not suitable for an efficient execution, since in order to determine the next step one usually has to iterate over the entire lattice and check for each site for all possible processes. Therefore a better scaling than $O(N)$, where N is the number of sites, cannot be achieved and the locality of the problem is wasted. But if one uses statements such as "If X diffuses from A to B, other diffusion from neighboring sites to A is enabled and diffusion from neighboring sites to B is disabled." one exploits the fact that chemical processes are strongly localized and an $O(1)$ scaling can be achieved. Considering the fact that the time evolution at each kMC step is proportional to $(k_{tot})^{-1}$, where k_{tot} is the total rate, the whole program scales linearly with N but each step only takes a constant time! This trick is known as local update algorithm. [47, 95]

Unfortunately experience shows that the implementation of such a local update formulation is laborious and error-prone for any but the simplest process lists. This manual translation process can be simplified if all two-site-processes such as diffusion or reaction are expressed in terms of lifting a particle and placing a particle on the lattice. It is then easier to write functions describing the effect of these more elementary steps. Still the complexity of each of these steps still grows at least linearly with the length of the process list. This means that it eventually becomes very involved to expand a model with more than a few dozen processes, since in this formulation every process virtually affects every other process.

As a solution a generic scheme was developed with the same basic structure as the description given in Appendix B but using XML[1]. Alongside a program was developed, which parses such a process list XML file, translates it to the local updating formulation, and writes a compiled language code (in this case FORTRAN90). This code in turn can be compiled and allows efficient execution.

This XML scheme has several benefits by itself. One automatically gains several advantages of XML schemes. A process list XML file compactly and unambiguously defines a kMC model in a platform independent way. One can store and exchange models conveniently. The programming time is drastically reduced and errors are often detected very early.
Additional fields such as rates can be added and together with a suitable XSLT[2] file a program becomes practically self-documenting.

INPUT/OUTPUT The fourth module bundles all input and output during runtime. The rate constants are calculated and assigned here as well as all parameters and calculated observables. This was usually implemented as a Python script, which interfaces with other modules

1 XML stands for Extensible Markup Language, see *e.g.* [96]
2 XSLT stands for Extensible Stylesheet Language Transformations

written in FORTRAN with the help of f2py. F2py is a useful tool to build such an interface. [97]

In summary I hope to have demonstrated that in this approach both aspects of efficiency are addressed rigorously. I would like to invite anyone to use and contribute to this project.[3]

3 All code is under GNU/GPL and available from `http://github.com/mhoffman/kMC_generator`.

B

KMC PROCESS LISTS

In this appendix the kMC process lists are stated including all parameters.

Description Scheme

The proposed kinetic Monte Carlo (kMC) process list for the Pd(100) phase of CO oxidation is explained here in a formalized way. Each elementary process will be stated as follows:

{Diagrams} {species} can {adsorb | desorb | diffuse | react } { {on | from | to} {sites...} }
if {condition 1 } [and
{condition 2}
...]
with {rate constant specifier} = {formula}
where
{explanation of symbols}.

B.1 PDO

The diagrams used below depict PdO bridge and hollow sites and are assigned as in figure 24. If not noted otherwise all barriers are taken from [27].

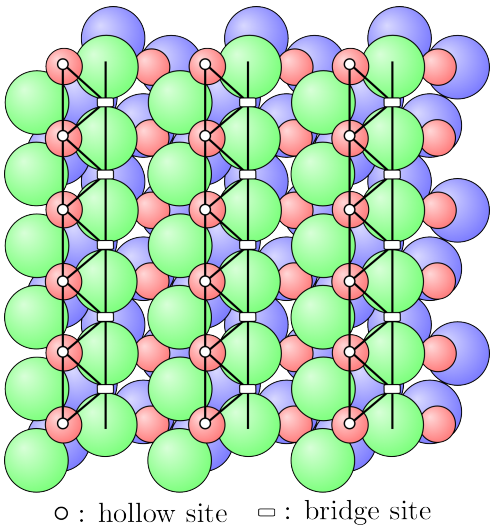

Figure 24: The assignment of adsorption sites to PdO

Process List

CO Adsorption

CO can adsorb on a if a is empty with

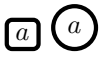

(a) (b)

Figure 25: Geometries for CO adsorption

$$k_{\mathrm{CO}}^{\mathrm{ads}} = \frac{p_{\mathrm{CO}} A}{\sqrt{2\pi m_{\mathrm{CO}} k_B T}}$$

where

- p_{CO}: CO partial pressure in bar
- A: $\frac{1}{2} A_{\left(\sqrt{5}\times\sqrt{5}\right)R27^\circ} = 19.47\,10^{-20}\mathrm{m}$
- m_{CO}: $4.6496\,10^{-26}\mathrm{kg}$
- k_B: $1.38065\,10^{-23}\mathrm{J\ K^{-1}}$
- T: temperature in K

O_2 Adsorption

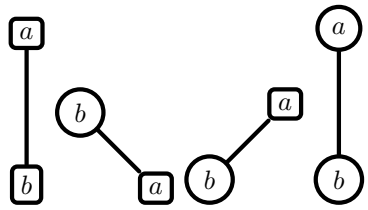

(a) (b) (c) (d)

Figure 26: Geometries for O_2 adsorption

O_2 can adsorb on a and b if a is empty and b is empty with

$$k_{\mathrm{O_2}}^{\mathrm{ads}} = \frac{p_{\mathrm{O_2}} A}{\sqrt{2\pi m_{\mathrm{O_2}} k_B T}} e^{-\beta E_{\mathrm{O_2}}^{\mathrm{diss}}}$$

where

- $E_{\mathrm{O_2}}^{\mathrm{diss}}$: -1.9eV dissociation barrier for bridge-bridge and 0eV otherwise

CO Desorption

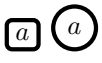

(a) (b)

Figure 27: Geometries for CO desorption

CO can desorb from a if a is occupied by CO with

$$k_{CO}^{des} = k_{CO}^{ads} e^{-\beta\left(\mu_{CO} - E_{CO}^{bind}\right)}$$

where

- μ_{CO}: chemical potential of gaseous CO
- $E_{CO}^{bind,hollow} = -1.88$eV, $E_{CO}^{bind,bridge}$: -1.45eV

O_2 Desorption

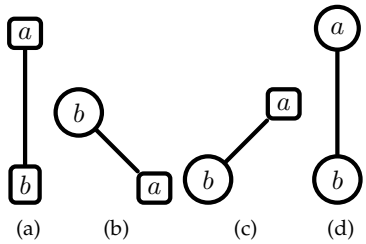

Figure 28: Geometries for O_2 desorption

O_2 can desorb from a and b if a is occupied by O and b is occupied by O with

$$k_{O_2}^{des} = k_{O_2}^{ads} e^{-\beta\left(\mu_{O_2} - \left(E_O^{bind,a} + E_{O_2}^{bind,b}\right)\right)}$$

where

- μ_{O_2} :chemical potential of gaseous O_2
- $E_O^{bind,hollow} = -1.97$eV,$E_O^{bind,bridge} = -0.43$eV

CO Diffusion

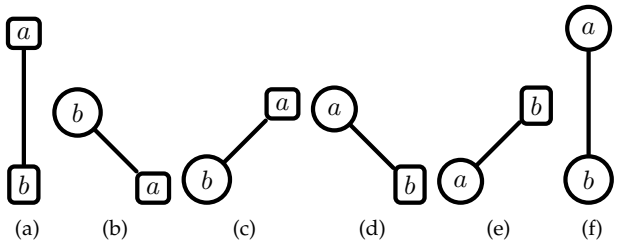

Figure 29: Geometries for CO diffusion

CO can diffuse from a to b if a is occupied by CO and b is empty with

$$k_{CO}^{diff} = (\beta h)^{-1} e^{-\beta\left(E_{CO}^{diff,a,b} + \max\left(0, E_{CO}^{bind,b} - E_{CO}^{bind,a}\right)\right)}$$

where

- $E_{CO}^{diff,bridge,hollow} = 0.3$eV

- $E_{\mathrm{CO}}^{\mathrm{diff,bridge,bridge}} = 0.4\mathrm{eV}$
- $E_{\mathrm{CO}}^{\mathrm{diff,hollow,hollow}} = 0.6\mathrm{eV}$

O Diffusion

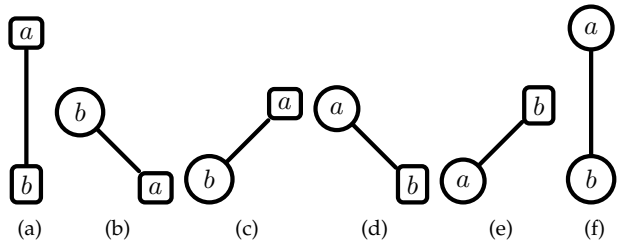

Figure 30: Geometries for CO diffusion

O can diffuse from a to b if a is occupied by O and b is empty with

$$k_{\mathrm{O}}^{\mathrm{diff}} = (\beta h)^{-1}\, \mathrm{e}^{-\beta\left(E_{\mathrm{O}}^{\mathrm{diff,a,b}} + \max\left(0, E_{\mathrm{O}}^{\mathrm{bind},b} - E_{\mathrm{O}}^{\mathrm{bind},a}\right)\right)}$$

where

- $E_{\mathrm{O}}^{\mathrm{diff,bridge,hollow}} = 0.1\mathrm{eV}$
- $E_{\mathrm{O}}^{\mathrm{diff,bridge,bridge}} = 1.2\mathrm{eV}$
- $E_{\mathrm{O}}^{\mathrm{diff,hollow,hollow}} = 1.4\mathrm{eV}$

Reaction

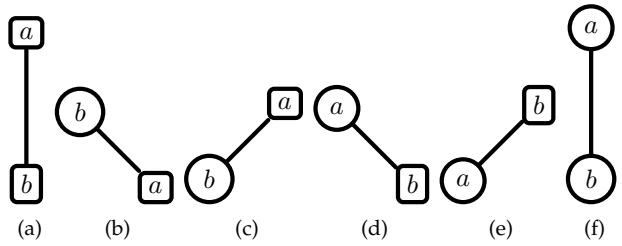

Figure 31: Geometries for CO diffusion

O+CO can react on a and b if a is occupied by O and b is occupied by CO with

$$k_{\mathrm{react}}^{\mathrm{O}a,\mathrm{CO}b} = (\beta h)^{-1}\, \mathrm{e}^{-\beta E_{\mathrm{react}}^{\mathrm{O}a,\mathrm{CO}b}}$$

where

- $E_{\mathrm{react}}^{\mathrm{Ohollow,CObridge}} = 0.8\mathrm{eV}$
- $E_{\mathrm{react}}^{\mathrm{Obridge,COhollow}} = 0.5\mathrm{eV}$
- $E_{\mathrm{react}}^{\mathrm{Obridge,CObridge}} = 1.0\mathrm{eV}$[28]
- $E_{\mathrm{react}}^{\mathrm{Ohollow,COhollow}} = 1.6\mathrm{eV}$[28]

B.2 PD(100)

The diagrams used below depict Pd(100) bridge and hollow sites and are assigned as in figure 32.

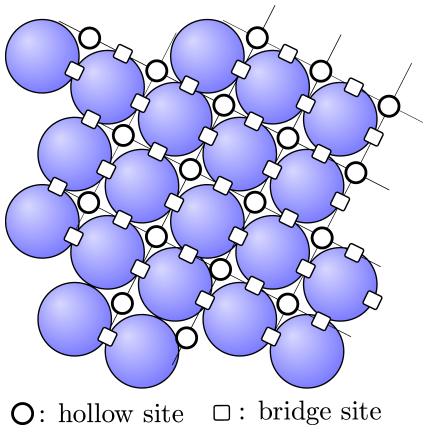

Figure 32: The assignment of adsorption sites to Pd(100).

Process List

CO Adsorption

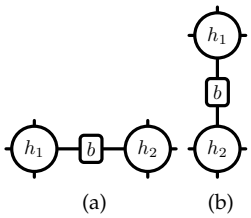

Figure 33: Geometries for CO adsorption.

CO can adsorb on b if h_1 is empty and h_2 is empty with

$$k_{\mathrm{CO}}^{\mathrm{ads}} = \frac{p_{\mathrm{CO}} A}{\sqrt{2\pi m_{\mathrm{CO}} k_B T}}$$

where

- p_{CO}: CO partial pressure in bar
- A: $\frac{(3.95\,10^{-10}\mathrm{m})^2}{2} = 7.80\,10^{-20}\mathrm{m}^2$[27][1]
- m_{CO}: $4.6496\,10^{-26}$kg
- k_B: $1.38065\,10^{-23}\mathrm{J\ K}^{-1}$
- T: temperature in K

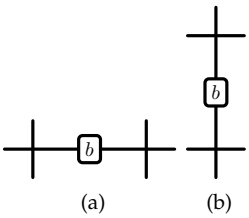

Figure 34: Geometries for CO desorption.

O_2 Adsorption-not included

CO Desorption

CO can desorb from b if b is occupied by CO with

$$k_{\mathrm{CO}}^{\mathrm{des}} = k_{\mathrm{CO}}^{\mathrm{ads}} \mathrm{e}^{-\beta\left(\mu_{\mathrm{CO}} - E_{\mathrm{CO}}^{\mathrm{bind}}\right)}$$

where:

- μ_{CO}: chemical potential of gaseous CO [98]
- $E_{\mathrm{CO}}^{\mathrm{bind}}$:-1.31eV from [27] PBE.

O_2 Desorption-not included

CO Diffusion

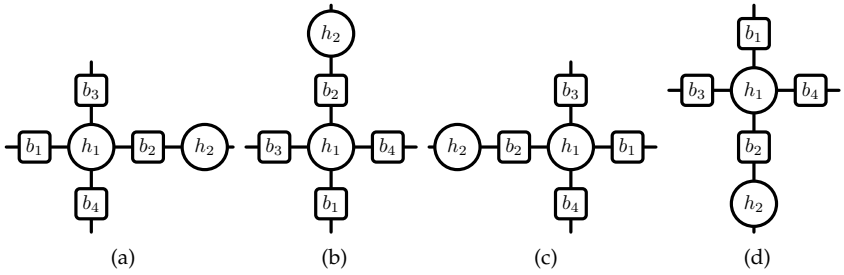

Figure 35: Geometries for CO diffusion (1).

CO can diffuse from b_1 to b_2 if b_1 is occupied by CO and h_1 is empty and b_2 is empty and b_3 is empty and b_4 is empty and h_2 is empty with

$$k_{\mathrm{CO}}^{\mathrm{diff}} = (\beta h)^{-1} \mathrm{e}^{-\beta E_{\mathrm{CO}}^{\mathrm{diff}}}$$

where

- h: $6.626\,10^{-34}$ J $\cdot$ s
- $E_{\mathrm{CO}}^{\mathrm{diff}} = E_{\mathrm{CO}}^{\mathrm{hollow}} - E_{\mathrm{CO}}^{\mathrm{bridge}} = (-0.83 \text{ eV }) - (-1.31 \text{ eV}) = 0.48 \text{ eV}$.[27]

CO can diffuse from b_1 to b_2 if b_1 is occupied by CO and h_1 is empty and b_2 is empty and h_2 is empty with

$$k_{\mathrm{CO}}^{\mathrm{diff}} \text{ (s. a.)}$$

1 One can assign two bridge sites to each unit cell, which has a lattice constant of $3.95\,10^{-10}$m as calculated with PBE in [27].

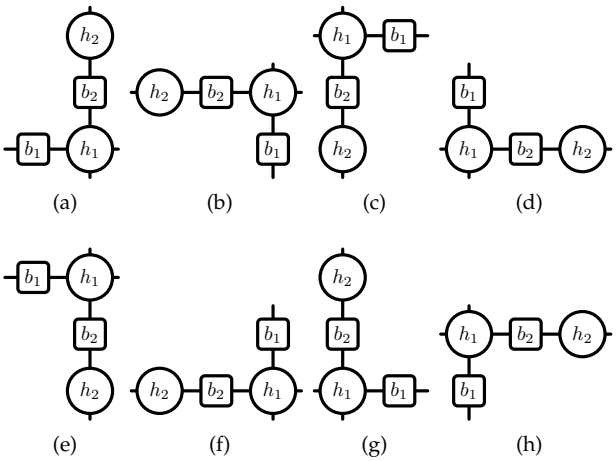

Figure 36: Geometries for CO diffusion (2).

O Diffusion-not included

Reaction-not included

[1] J. J. Berzelius, L. F. Svanberg, and K. S. vetenskapsakademien, 1835. *Jahres-Bericht über die Fortschritte der Chemie*. H. Laupp.

[2] G. Centi and R. A. van Santen, 2007. *Catalysis for Renewables: From Feedstock to Energy Production*. Wiley-VCH, ISBN:3527317880.

[3] G. Ertl, H. Knözinger, and J. Weitkamp, 1999. *Preparation of solid catalysts*. Wiley-VCH, ISBN:9783527298266.

[4] B. Cornils, W. A. Herrmann, R. Schlögl, and C. Wong, 2003. *Catalysis from A to Z: A Concise Encyclopedia*. Wiley-VCH, 2., vollst. überarb. und erw. a. 2003. edition, ISBN:3527303731.

[5] J. Fish, 2009. *Multiscale Methods: Bridging the Scales in Science and Engineering*. Oxford University Press, ISBN:9780199233854.

[6] A. Brandt, J. Bernholc, and K. Binder, 2001. *Multiscale computational methods in chemistry and physics*. IOS Press, ISBN:9781586031411.

[7] S. Attinger and P. D. Koumoutsakos, 2004. *Multiscale modelling and simulation*. Springer, ISBN:9783540211808.

[8] R. A. Santen and M. Neurock, 2006. *Molecular heterogeneous catalysis: a conceptual and computational approach*. Wiley-VCH, ISBN:9783527296620.

[9] K. Reuter, 2009. *First-principles kinetic Monte Carlo simulations for heterogeneous catalysis: Concepts, status and frontiers*.

[10] R. K. Pathria, 1996. *Statistical mechanics*. Butterworth-Heinemann, ISBN:9780750624695.

[11] C. Stampfl, 1997. *Study of CO oxidation over Ru(0001) at high gas pressures*. Surface Science, **377**:808–812.

[12] J. K. Norskov, T. Bligaard, J. Rossmeisl, and C. H. Christensen, 2009. *Towards the computational design of solid catalysts*. Nat Chem, **1**(1):37–46, doi:10.1038/nchem.121.

[13] R. Goeke and A. Datye, 2007. *Model oxide supports for studies of catalyst sintering at elevated temperatures*. Topics in Catalysis, **46**(1):3–9, doi:10.1007/s11244-007-0309-5.

[14] P. Marécot, A. Akhachane, and J. Barbier, 1996. *Coke deposition on supported palladium catalysts*. Catalysis Letters, **36**(1):37–39, doi:10.1007/BF00807203.

[15] E. E. Wolf and F. Alfani, 1982. *Catalysts Deactivation by Coking*. Catalysis Reviews: Science and Engineering, **24**(3):329, doi:10.1080/03602458208079657.

[16] M. Shelef and R. W. McCabe, 2000. *Twenty-five years after introduction of automotive catalysts: what next?* Catalysis Today, **62**(1):35–50, doi:10.1016/S0920-5861(00)00407-7.

[17] H. S. Gandhi, G. W. Graham, and R. W. McCabe, 2003. *Automotive exhaust catalysis*. Journal of Catalysis, **216**(1-2):433–442, doi:10.1016/S0021-9517(02)00067-2.

[18] F. Haaß and H. Fuess, 2005. *Structural Characterization of Automotive Catalysts*. Advanced Engineering Materials, **7**(10):899–913, doi:10.1002/adem.200500120.

[19] S. Chang and P. A. Thiel, 1988. *Summary Abstract: Temperature- and coverage-dependent structures of oxygen on Pd(100)*. Journal of Vacuum Science & Technology A: Vacuum, Surfaces, and Films, **6**(3):837–839, doi:10.1116/1.575082.

[20] S. Chang, P. Thiel, and J. Evans, 1988. *Oxygen-stabilized reconstructions of Pd(100): Phase transitions during oxygen desorption*. Surface Science, **205**(1-2):117–142, doi:10.1016/0039-6028(88)90167-7.

[21] E. Stuve, R. Madix, and C. Brundle, 1985. *The adsorption and reaction of ethylene on clean and oxygen covered Pd(100)*. Surface Science, **152-153**(PART 1):532–542.

[22] T. Orent and S. Bader, 1982. *LEED and ELS study of the initial oxidation of Pd(100)*. Surface Science, **115**(2):323–334, doi:10.1016/0039-6028(82)90412-5.

[23] M. Todorova, E. Lundgren, V. Blum, A. Mikkelsen, S. Gray, J. Gustafson, M. Borg, J. Rogal, K. Reuter, J. N. Andersen, and M. Scheffler, 2003. *The Pd(1 0 0)-R27°-O surface oxide revisited*. Surface Science, **541**(1-3):101–112, doi:10.1016/S0039-6028(03)00873-2.

[24] E. Lundgren, A. Mikkelsen, J. N. Andersen, G. Kresse, M. Schmid, and P. Varga, 2006. *Surface oxides on close-packed surfaces of late transition metals*. Journal of Physics: Condensed Matter, **18**(30):R481–R499.

[25] P. Kostelník, N. Seriani, G. Kresse, A. Mikkelsen, E. Lundgren, V. Blum, T. Sikola, P. Varga, and M. Schmid, 2007. *The surface oxide: A LEED, DFT and STM study*. Surface Science, **601**(6):1574–1581, doi:10.1016/j.susc.2007.01.026.

[26] M. Todorova, 2004. *Oxidation of palladium surfaces*. Berlin, Techn. Univ., Diss., 2004.

[27] J. Rogal, 2006. *Stability, Composition and Function of Palladium Surfaces in Oxidizing Environments*. Ph.D. thesis, FU Berlin.

[28] J. Rogal, K. Reuter, and M. Scheffler, 2008. *CO oxidation on Pd(100) at technologically relevant pressure conditions: First-principles kinetic Monte Carlo study*. Physical Review B (Condensed Matter and Materials Physics), **77**(15):155410–12, doi:10.1103/PhysRevB.77.155410.

[29] J. Rogal, K. Reuter, and M. Scheffler, 2007. *CO oxidation at Pd(100): A first-principles constrained thermodynamics study*. Physical Review B, **75**(20), doi:10.1103/PhysRevB.75.205433.

[30] B. Hendriksen, S. Bobaru, and J. Frenken, 2004. *Oscillatory CO oxidation on Pd(100) studied with in situ scanning tunneling microscopy*. Surface Science, **552**(1-3):229–242, doi:10.1016/j.susc.2004.01.025.

[31] M. Chen, Y. Cai, Z. Yan, K. Gath, S. Axnanda, and D. Goodman, 2007. *Highly active surfaces for CO oxidation on Rh, Pd, and Pt*. Surface Science, **601**(23):5326–5331, doi:10.1016/j.susc.2007.08.019.

[32] S. M. McClure and D. W. Goodman, 2009. *New insights into catalytic CO oxidation on Pt-group metals at elevated pressures*. Chemical Physics Letters, **469**(1-3):1–13, doi:10.1016/j.cplett.2008.12.066.

[33] B. Hendriksen, S. Bobaru, and J. Frenken, 2005. *Looking at Heterogeneous Catalysis at Atmospheric Pressure Using Tunnel Vision*. Topics in Catalysis, **36**(1):43–54, doi:10.1007/s11244-005-7861-7.

[34] F. Gao, Y. Wang, and D. W. Goodman, 2010. *Reply to "Comment on 'CO Oxidation on Pt-Group Metals from Ultrahigh Vacuum to Near Atmospheric Pressures. 2. Palladium and Platinum'"*. The Journal of Physical Chemistry C, **114**(14):6874, doi:10.1021/jp100134e.

[35] R. van Rijn, O. Balmes, R. Felici, J. Gustafson, D. Wermeille, R. Westerström, E. Lundgren, and J. W. M. Frenken, 2010. *Comment on "CO Oxidation on Pt-Group Metals from Ultrahigh Vacuum to Near Atmospheric Pressures. 2. Palladium and Platinum"*. The Journal of Physical Chemistry C, **114**(14):6875–6876, doi:10.1021/jp911406x.

[36] K. Reuter and M. Scheffler, 2003. *First-Principles Atomistic Thermodynamics for Oxidation Catalysis: Surface Phase Diagrams and Catalytically Interesting Regions*. Physical Review Letters, **90**(4):046103, doi:10.1103/PhysRevLett.90.046103.

[37] R. M. Ziff, E. Gulari, and Y. Barshad, 1986. *Kinetic Phase Transitions in an Irreversible Surface-Reaction Model*. Physical Review Letters, **56**(24):2553, doi:10.1103/PhysRevLett.56.2553.

[38] D. Frenkel, 2002. *Understanding molecular simulation : from algorithms to applications*. Academic Press, San Diego, 2nd ed. edition, ISBN:9780122673511.

[39] D. P. Landau and K. Binder, 2009. *A Guide to Monte Carlo Simulations in Statistical Physics*. Cambridge University Press, 3 edition, ISBN:0521768489.

[40] C. Gardiner, 2004. *Handbook of Stochastic Methods: for Physics, Chemistry and the Natural Sciences*. Springer, 3rd edition, ISBN:3540208828.

[41] P. W. H, T. S. A, V. W. T, and F. B. P, 2007. *Numerical Recipes 3rd Edition: The Art of Scientific Computing*. Cambridge University Press, 3 edition, ISBN:0521880688.

[42] A. B. Bortz, M. H. Kalos, and J. L. Lebowitz, 1975. *A new algorithm for Monte Carlo simulation of Ising spin systems*. Journal of Computational Physics, **17**(1):10–18, doi:10.1016/0021-9991(75)90060-1.

[43] D. T. Gillespie, 1976. *A general method for numerically simulating the stochastic time evolution of coupled chemical reactions*. Journal of Computational Physics, **22**(4):403–434, doi:10.1016/0021-9991(76)90041-3.

[44] K. A. Fichthorn and W. H. Weinberg, 1991. *Theoretical foundations of dynamical Monte Carlo simulations*. The Journal of Chemical Physics, **95**(2):1090–1096, doi:10.1063/1.461138.

[45] E. Machado, G. M. Buendia, P. A. Rikvold, and R. M. Ziff, 2005. *Response of a catalytic reaction to periodic variation of the CO pressure: Increased C O2 production and dynamic phase transition*. Physical Review E, **71**(1):016120, doi:10.1103/PhysRevE.71.016120.

[46] R. M. Ziff, E. Gulari, and Y. Barshad, 1986. *Kinetic Phase Transitions in an Irreversible Surface-Reaction Model*. Physical Review Letters, **56**(24):2553, doi:10.1103/PhysRevLett.56.2553.

[47] A. Chatterjee and D. G. Vlachos, 2007. *An overview of spatial microscopic and accelerated kinetic Monte Carlo methods*. Journal of Computer-Aided Materials Design, **14**(2):253–308, doi:10.1007/s10820-006-9042-9.

[48] J. S. Reese, S. Raimondeau, and D. G. Vlachos, 2001. *Monte Carlo Algorithms for Complex Surface Reaction Mechanisms: Efficiency and Accuracy*. Journal of Computational Physics, **173**(1):302–321, doi:10.1006/jcph.2001.6877.

[49] D. Nicholson, 1984. *Grand Ensemble Monte Carlo*. http://www.ccp5.ac.uk/newsletter_index.shtml.

[50] A. P. J. Jansen, 2003. *An Introduction To Monte Carlo Simulations Of Surface Reactions*. cond-mat/0303028.

[51] A. F. Voter, 2007. *Introduction to the kinetic Monte Carlo method*. In *Radiation Effects in Solids*, p. 1–23.

[52] L. Xu and G. Henkelman, 2008. *Adaptive kinetic Monte Carlo for first-principles accelerated dynamics*. The Journal of Chemical Physics, **129**(11):114104, doi:10.1063/1.2976010.

[53] O. Trushin, H. Yildirim, A. Kara, and T. S. Rahman, 2008. *Off-Lattice Self-Learning Kinetic Monte Carlo: Application to 2D Cluster Diffusion on the fcc(111) Surface*. 0811.4375.

[54] O. Trushin, A. Karim, A. Kara, and T. S. Rahman, 2005. *Self-learning kinetic Monte Carlo method: Application to Cu(111)*. Physical Review B, **72**(11):115401, doi:10.1103/PhysRevB.72.115401.

[55] F. El-Mellouhi, N. Mousseau, and L. J. Lewis, 2008. *Kinetic activation-relaxation technique: An off-lattice self-learning kinetic Monte Carlo algorithm*. Physical Review B, **78**(15):153202, doi:10.1103/PhysRevB.78.153202.

[56] G. Henkelman and H. Jo?nsson, 1999. *A dimer method for finding saddle points on high dimensional potential surfaces using only first derivatives*. The Journal of Chemical Physics, **111**(15):7010, doi:10.1063/1.480097.

[57] G. T. Barkema and N. Mousseau, 1996. *Event-Based Relaxation of Continuous Disordered Systems*. Physical Review Letters, **77**(21):4358, doi:10.1103/PhysRevLett.77.4358.

[58] R. Malek and N. Mousseau, 2000. *Dynamics of Lennard-Jones clusters: A characterization of the activation-relaxation technique*. Physical Review E, **62**(6):7723, doi:10.1103/PhysRevE.62.7723.

[59] N. Mousseau, 2010. *private communications*.

[60] K. Reuter and M. Scheffler, 2005. *First-principles kinetic Monte Carlo simulations for heterogeneous catalysis, applied to the CO oxidation at RuO2(110)*. cond-mat/0510234, doi:doi:10.1103/PhysRevB.73.045433. Phys. Rev. B 73, 045433 (2005).

[61] K. Reuter, D. Frenkel, and M. Scheffler, 2004. *The Steady State of Heterogeneous Catalysis, Studied by First-Principles Statistical Mechanics*. Physical Review Letters, **93**(11):116105, doi:10.1103/PhysRevLett.93.116105.

[62] K. Reuter and M. Scheffler, 2003. *Composition and structure of the RuO2(110) surface in an O2 and CO environment: Implications for the catalytic formation of CO2*. Physical Review B, **68**(4):045407, doi:10.1103/PhysRevB.68.045407.

[63] G. L. Kellogg and P. J. Feibelman, 1990. *Surface self-diffusion on Pt(001) by an atomic exchange mechanism*. Physical Review Letters, **64**(26):3143, doi:10.1103/PhysRevLett.64.3143.

[64] C. Chen and T. T. Tsong, 1990. *Displacement distribution and atomic jump direction in diffusion of Ir atoms on the Ir(001) surface*. Physical Review Letters, **64**(26):3147, doi:10.1103/PhysRevLett.64.3147.

[65] F. Tao, S. Dag, L. Wang, Z. Liu, D. R. Butcher, H. Bluhm, M. Salmeron, and G. A. Somorjai, 2010. *Break-Up of Stepped Platinum Catalyst Surfaces by High CO Coverage*. Science, **327**(5967):850–853, doi:10.1126/science.1182122.

[66] H. Meskine, S. Matera, M. Scheffler, K. Reuter, and H. Metiu, 2009. *Examination of the concept of degree of rate control by first-principles kinetic Monte Carlo simulations*. Surface Science, **603**(10-12):1724–1730, doi:10.1016/j.susc.2008.08.036.

[67] B. Temel, H. Meskine, K. Reuter, M. Scheffler, and H. Metiu, 2007. *Does phenomenological kinetics provide an adequate description of heterogeneous catalytic reactions?* The Journal of Chemical Physics, **126**(20):204711, doi:10.1063/1.2741556. PMID: 17552793.

[68] P. Hänggi, P. Talkner, and M. Borkovec, 1990. *Reaction-rate theory: fifty years after Kramers*. Reviews of Modern Physics, **62**(2):251, doi:10.1103/RevModPhys.62.251.

[69] A. C. Gross, 2009. *Theoretical Surface Science: A Microscopic Perspective*. Springer, Berlin, 2nd ed. edition, ISBN:3540689664.

[70] R. I. Masel, 1996. *Principles of Adsorption and Reaction on Solid Surfaces*. John Wiley & Sons, 1. auflage edition, ISBN:0471303925.

[71] D. Chandler, 1987. *Introduction to modern statistical mechanics*. Oxford University Press, New York, ISBN:9780195042764.

[72] G. B. Arfken, H. J. Weber, and F. Harris, 2000. *Mathematical Methods for Physicists, Fifth Edition*. Academic Press, 5 edition, ISBN:0120598256.

[73] M. A. V. Hove, K. Hermann, and P. R. Watson, 2002. *The NIST Surface Structure Database – SSD version 4*. Acta Crystallographica Section B Structural Science, **58**(3):338–342, doi:10.1107/S0108768102002434.

[74] H. Huang and G. Gilmer, 1999. *Multi-lattice Monte Carlo model of thin films*. Journal of Computer-Aided Materials Design, **6**(2):117–127, doi:10.1023/A:1008722515055.

[75] C. Bos, F. Sommer, and E. J. Mittemeijer, 2004. *A kinetic Monte Carlo method for the simulation of massive phase transformations*. Acta Materialia, **52**(12):3545–3554, doi:10.1016/j.actamat.2004.04.008.

[76] C. Bos, 2004. *Atomistic simulation of interface controlled solid state phase transformations*. Ph.D. thesis, University Stuttgart.

[77] O. Kortlüke, V. N. Kuzovkov, and W. von Niessen, 1999. *Global Synchronization via Homogeneous Nucleation in Oscillating Surface Reactions*. Physical Review Letters, **83**(15):3089, doi:10.1103/PhysRevLett.83.3089.

[78] O. Kortlüke, V. N. Kuzovkov, and W. von Niessen, 1998. *Oscillation Phenomena Leading to Chaos in a Stochastic Surface Reaction Model*. Physical Review Letters, **81**(10):2164, doi:10.1103/PhysRevLett.81.2164.

[79] V. N. Kuzovkov, O. Kortlüke, and W. von Niessen, 2002. *Kinetic model for surface reconstruction*. Physical Review E, **66**(1):011603, doi:10.1103/PhysRevE.66.011603.

[80] V. N. Kuzovkov, O. Kortlüke, and W. von Niessen, 1999. *Nucleation and Island Growth Kinetics on Reconstructing Surfaces*. Physical Review Letters, **83**(8):1636, doi:10.1103/PhysRevLett.83.1636.

[81] O. Kortlüke, V. N. Kuzovkov, and W. von Niessen, 1999. *Simulation of kinetic oscillations in surface reactions on reconstructing surfaces*. The Journal of Chemical Physics, **110**(23):11523, doi:10.1063/1.479094.

[82] W. S. Epling, L. E. Campbell, A. Yezerets, N. W. Currier, and J. E. Parks, 2004. *Overview of the Fundamental Reactions and Degradation Mechanisms of NOx Storage/Reduction Catalysts*. Catalysis Reviews: Science and Engineering, **46**(2):163, doi:10.1081/CR-200031932.

[83] S. Reich, L. Li, and J. Robertson, 2006. *Control the chirality of carbon nanotubes by epitaxial growth*. Chemical Physics Letters, **421**(4-6):469–472, doi:10.1016/j.cplett.2006.01.110.

[84] J. Jelic and R. J. Meyer, 2009. *Density functional theory examination of Pd(111) and Pd(100) under NO oxidation conditions*. Physical Review B, **79**(12):125410, doi:10.1103/PhysRevB.79.125410.

[85] J. Quinn, Y. S. Li, D. Tian, H. Li, F. Jona, and P. M. Marcus, 1990. *Anomalous multilayer relaxation of Pd001*. Physical Review B, **42**(17):11348, doi:10.1103/PhysRevB.42.11348.

[86] R. J. Behm, K. Christmann, G. Ertl, and M. A. V. Hove, 1980. *Adsorption of CO on Pd(100)*. The Journal of Chemical Physics, **73**(6):2984, doi:10.1063/1.440430.

[87] A. M. Bradshaw and F. M. Hoffmann, 1978. *The chemisorption of carbon monoxide on palladium single crystal surfaces: IR spectroscopic evidence for localised site adsorption*. Surface Science, **72**(3):513–535, doi:10.1016/0039-6028(78)90367-9.

[88] G. Mills, H. Jónsson, and G. K. Schenter, 1995. *Reversible work transition state theory: application to dissociative adsorption of hydrogen*. Surface Science, **324**(2-3):305–337, doi:10.1016/0039-6028(94)00731-4.

[89] J. R. Lacher, 1937. *The Statistics of the Hydrogen-Palladium System*. Mathematical Proceedings of the Cambridge Philosophical Society, **33**(04):518–523, doi:10.1017/S0305004100077641.

[90] E. Lundgren, J. Gustafson, A. Mikkelsen, J. Andersen, A. Stierle, H. Dosch, M. Todorova, J. Rogal, K. Reuter, and M. Scheffler, 2004. *Kinetic Hindrance during the Initial Oxidation of Pd(100) at Ambient Pressures*. Physical Review Letters, **92**(4), doi:10.1103/PhysRevLett.92.046101.

[91] M. Todorova, K. Reuter, and M. Scheffler, 2005. *Density-functional theory study of the initial oxygen incorporation in Pd(111)*. Physical Review B, **71**(19), doi:10.1103/PhysRevB.71.195403.

[92] S. Y. Kim, I. Lee, and S. Jun, 2007. *Transition-pathway models of atomic diffusion on fcc metal surfaces. I. Flat surfaces*. Physical Review B (Condensed Matter and Materials Physics), **76**(24):245407–15, doi:10.1103/PhysRevB.76.245407.

[93] S. Y. Kim, I. Lee, and S. Jun, 2007. *Transition-pathway models of atomic diffusion on fcc metal surfaces. II. Stepped surfaces*. Physical Review B (Condensed Matter and Materials Physics), **76**(24):245408–20, doi:10.1103/PhysRevB.76.245408.

[94] G. Wilson, 2006. *Where's the Real Bottleneck in Scientific Computing?* American Scientist, **94**(1):5, doi:10.1511/2006.1.5.

[95] J. S. Reese, S. Raimondeau, and D. G. Vlachos, 2001. *Monte Carlo Algorithms for Complex Surface Reaction Mechanisms: Efficiency and Accuracy*. Journal of Computational Physics, **173**(1):302–321, doi:10.1006/jcph.2001.6877.

[96] E. R. Harold and W. S. Means, 2004. *XML in a Nutshell, Third Edition*. O'Reilly Media, 3 edition, ISBN:0596007647.

[97] H. P. Langtangen, 2009. *A Primer on Scientific Programming with Python*. Springer, Berlin, 1 edition, ISBN:3642024742.

[98] J. Rogal and K. Reuter, 2006. *Ab Initio Atomistic Thermodynamics for Surfaces: A Primer*. Technical report.

ACKNOWLEDGMENTS

I would like to thank Karsten Reuter for being a terrific advisor and mentor. I also would like to thank Matthias Scheffler for all the support and for suggesting such an intriguing topic. Special thanks go to Jelena Jelic for the DFT calculations and many discussions in the beginning of the project as well as to Jutta Rogal for providing the kMC of her thesis. Kudos go to Jörg Meyer, who is so kind to share his giftedness. I would also like to thank Matthias Gramzow, Mathis Gruber, Matteo Maestri, Sebastian Matera, Michael Rieger, Erik McNellis, and everyone from the theory department.

This work would not have been possible without really good teachers of which I would like to thank in particular Bodo Hamprecht, Hardy Gross, Stefan Kurth, Andreas Ludwig, Horia Metiu, and Friedrich Minde.

I would like to thank my parents for all their support and for financing my studies. And finally it's all moot without good friends who supported me along the way. Thanks go to Juscele Duraes, Antonia Aravena, Ulrich Beier, Christopher Bronner, Heiko Dumlich, Frank Essenberger, Torsten Karzig, Andreas Linscheid, Robert Nordvall, Leighton Rice, Kai Schmitz, Torsten Silow, Maxie Müller, Daniel Sank, and Nils Kurschat—I will never forget.

DECLARATION

I hereby declare that I produced this diploma thesis without external assistance, and that no other than the listed references have been used as sources of information.
Berlin, June 2010

Max J. Hoffmann